POST-MERGER OSCILLATIONS AND THE NEWCOMPSTAR ACTION

NIKOLAOS STERGIOULAS

DEPARTMENT OF PHYSICS
ARISTOTLE UNIVERSITY OF THESSALONIKI

Seattle, July 1, 2014

Plan of Talk

Part I: Understanding post-merger oscillations

Mon. Not. R. Astron. Soc. **418,** 427–436 (2011)

Gravitational waves and non-axisymmetric oscillation modes in mergers of compact object binaries

Nikolaos Stergioulas,[1★] Andreas Bauswein,[2] Kimon Zagkouris[1]
and Hans-Thomas Janka[2]

Part II: Extracting EOS information

arxiv:1403.5301, Phys. Rev. D, in press (2014)

Revealing the high-density equation of state through binary neutron star mergers

A. Bauswein,[1] N. Stergioulas,[1] and H.-T. Janka[2]

Part III: Towards hybrid waveforms

arxiv:1406.5444, submitted to Phys. Rev. D (2014)

Prospects For High Frequency Burst Searches Following Binary Neutron Star Coalescence With Advanced Gravitational Wave Detectors

J. Clark,[1] A. Bauswein,[2] L. Cadonati,[1,3] H.-T. Janka,[4] C. Pankow,[5] and N. Stergioulas[2]

PART I:

UNDERSTANDING POST-MERGER OSCILLATIONS

Outcome of Binary NS Mergers

(Hotokezaka et al., 2011)
(Bauswein & Janka, 2012)

Most likely range of masses for binary system:

$$2.7\,M_{sun} < M_{tot} < 2.8\,M_{sun}$$

If EOS has nonrotating $M_{max} > 2\,M_{sun}$ (as required by observations), then a long-lived ($\tau > 10$ms) remnant is formed.

The remnant is a *hypermassive neutron star (HMNS)*, supported by *differential rotation*, with a mass larger than the maximum mass allowed for uniform rotation.

The GW signal can be divided into three distinct phases: *inspiral*, *merger* and *post-merger ringdown*.

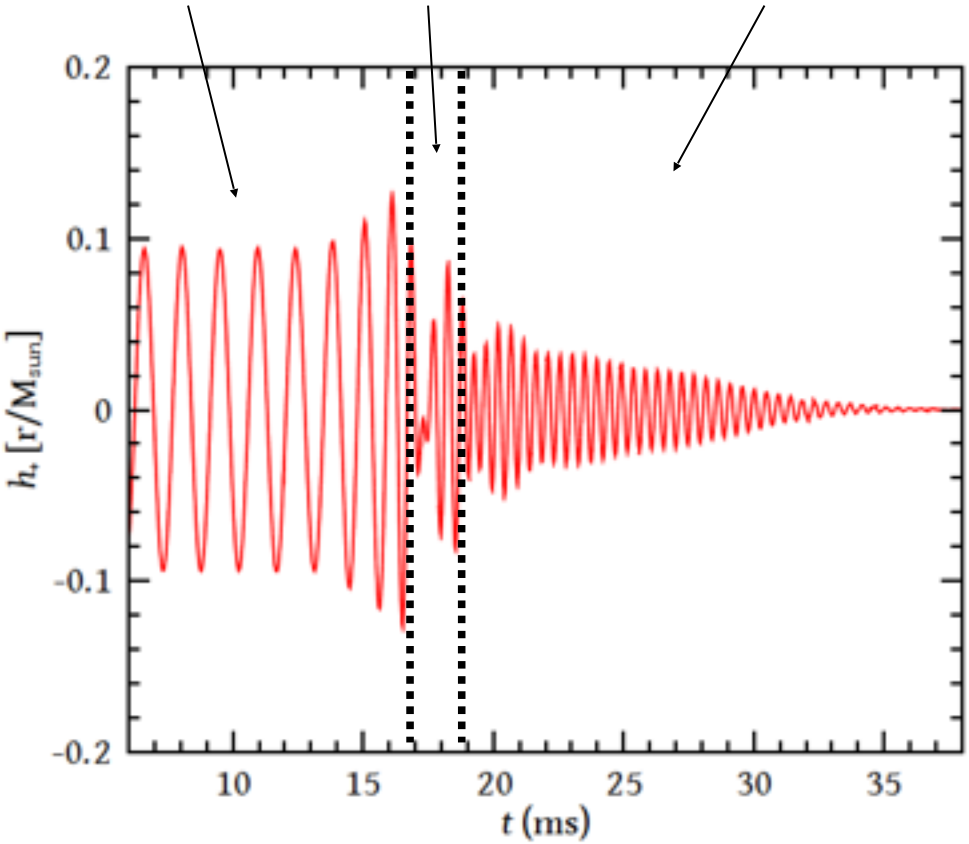

@40Mpc

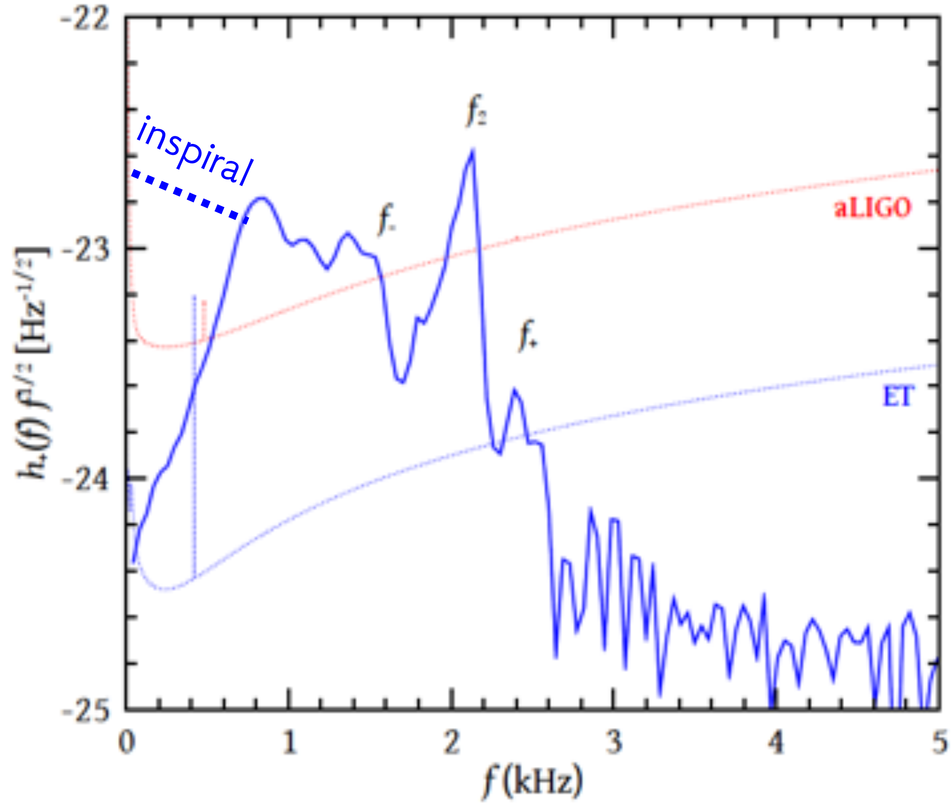

Several peaks stand above the aLIGO/VIRGO or ET sensitivity curves and are potentially detectable. Are these *oscillations* of the HMNS?

Additional EOS Information in Post-Merger Signal

How can we interpret the triplet of frequencies above the ET sensitivity curve?

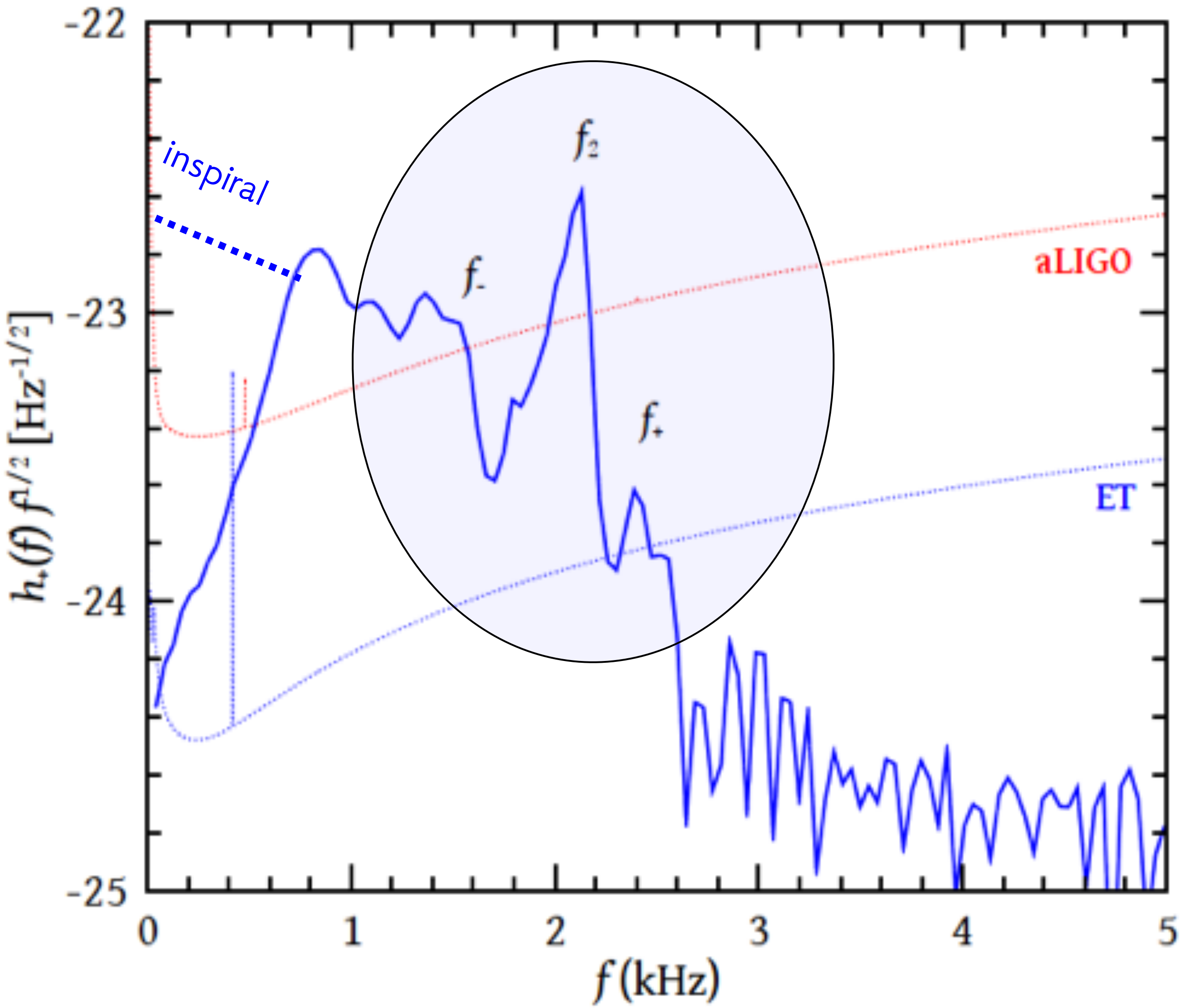

Mergers of Compact Object Binaries

NS, Bauswein, Zagkouris, Janka (2011)

Merger of equal/unequal mass binaries with *LS*, *Shen*, *MIT60* EOS. (3-D GR CFC/SPH code) Example: Shen EOS: $1.35M_{sun}+1.35M_{sun}$

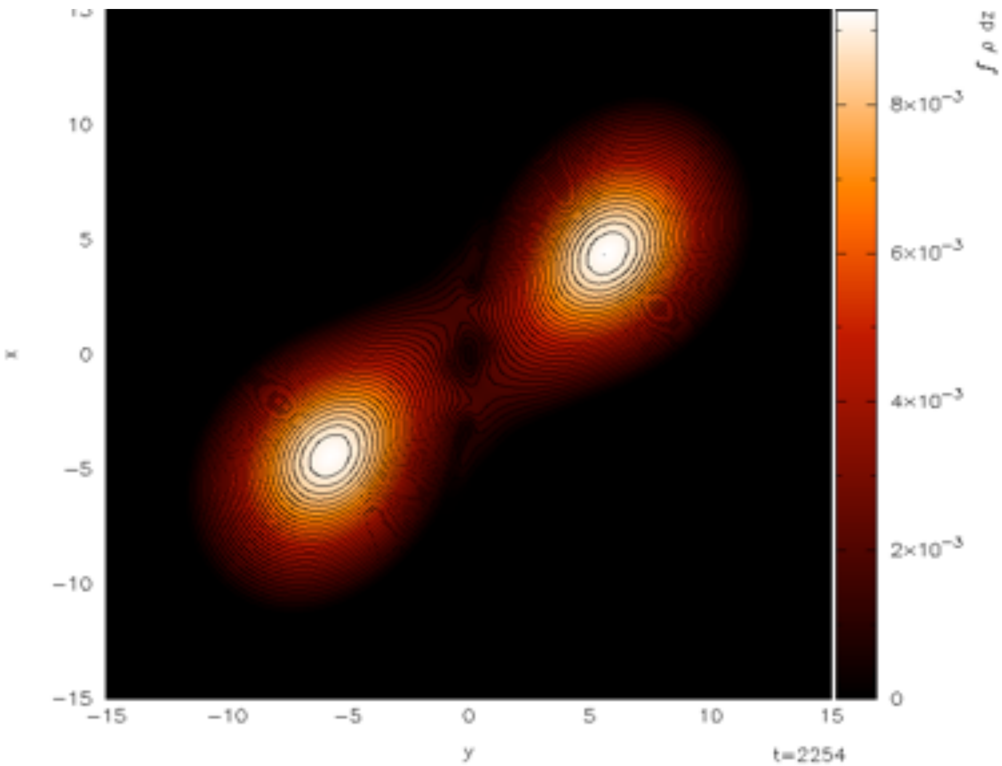

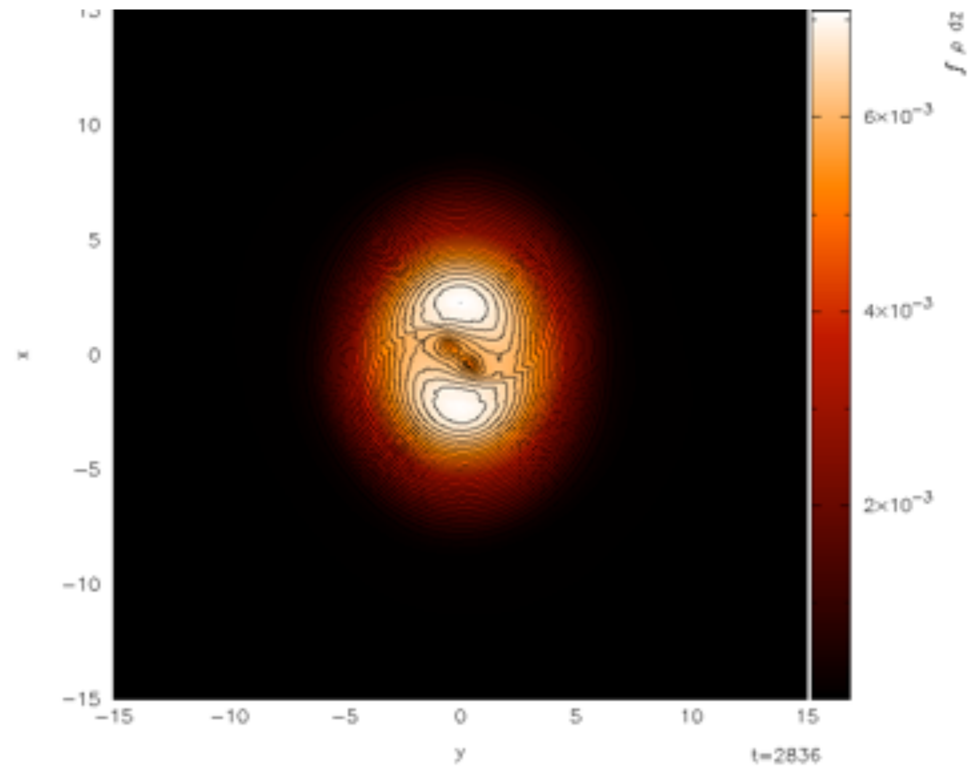

Rotating bar shape + *radial oscillation* => *transient double core*

GW Scaled Power Spectral Density

Split the time-series into *pre-merger* and *post-merger* parts:

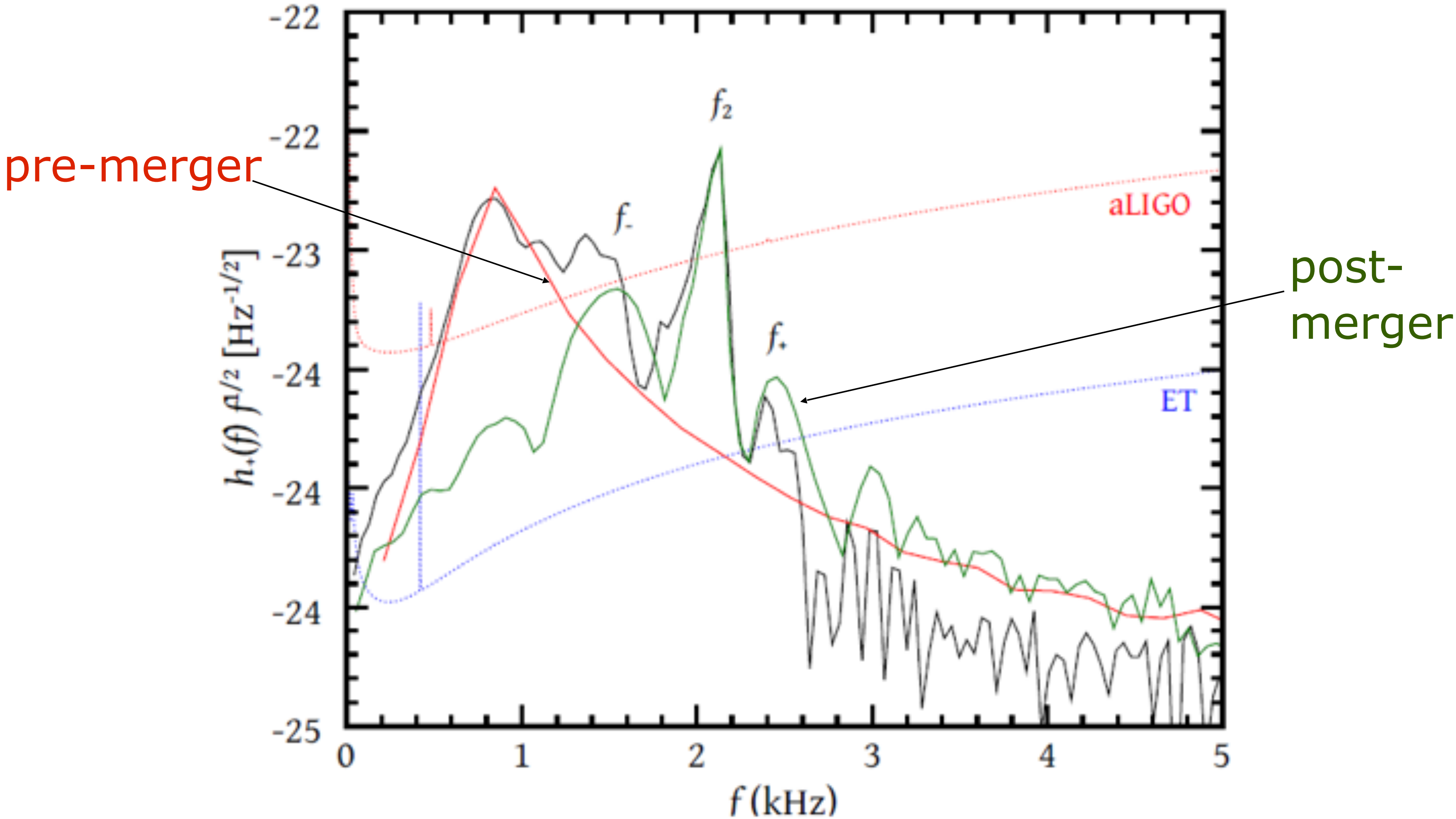

Triplet of frequencies: *f_- , f_2 , f_+ originates in post-merger part.*

Nonlinear Combination Frequencies

Passamonti, NS & Nagar (2007)

Linear sums and differences of linear mode frequencies

$$f^{\pm} = {}^2f \pm F \qquad p_n^{\pm} = {}^2p_n \pm F \qquad H_n^{\pm} = H_n \pm {}^2f$$

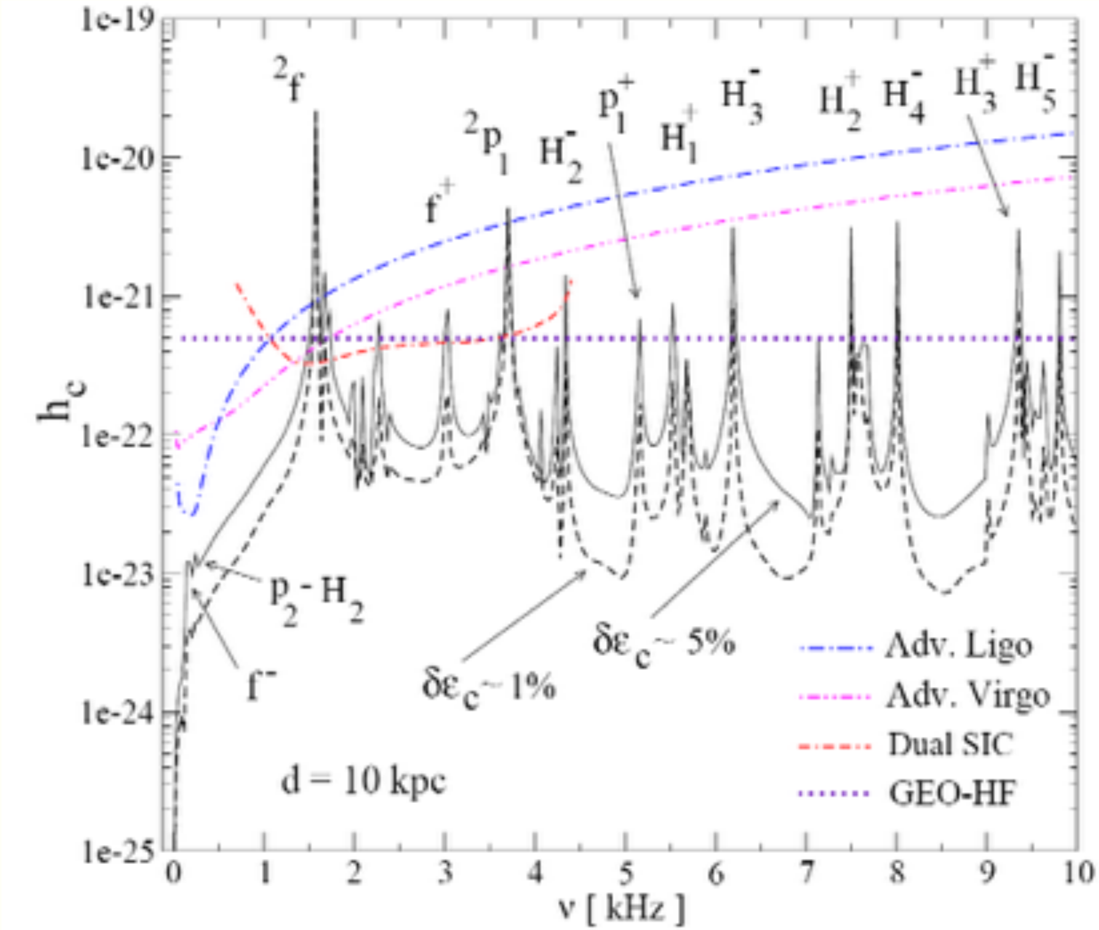

The amplitude of combination frequencies can become large, when the linear modes have amplitude of $O(1)$.

Equal mass: Lattimer-Swesty 1.35+1.35

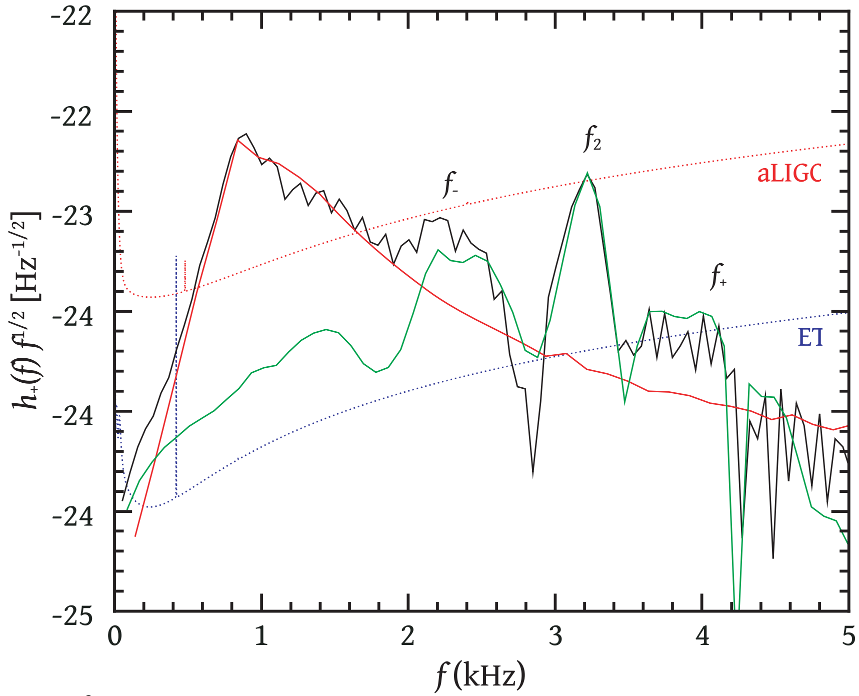

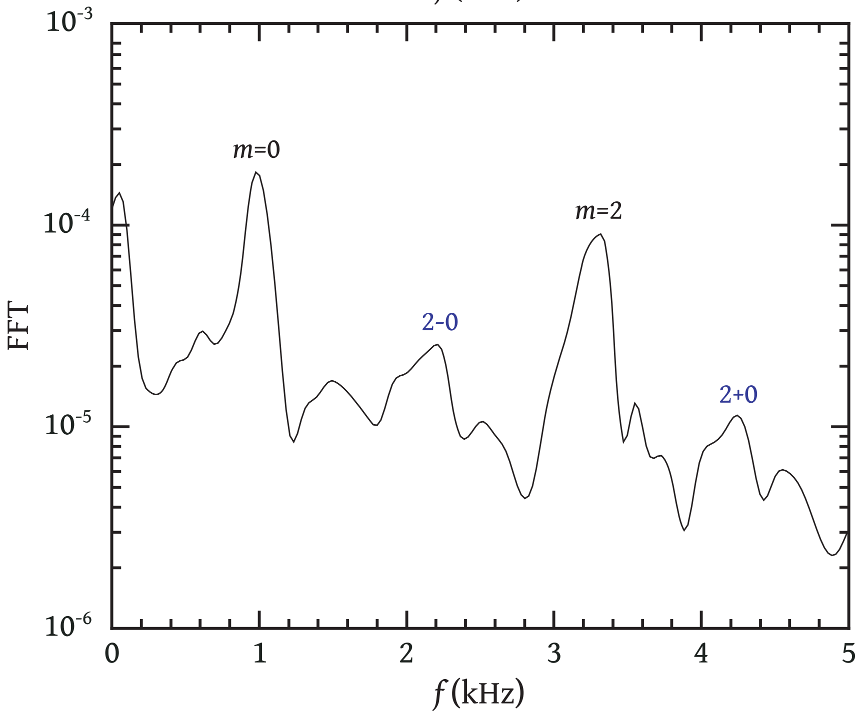

Unequal mass: Lattimer-Swesty 1.2+1.35

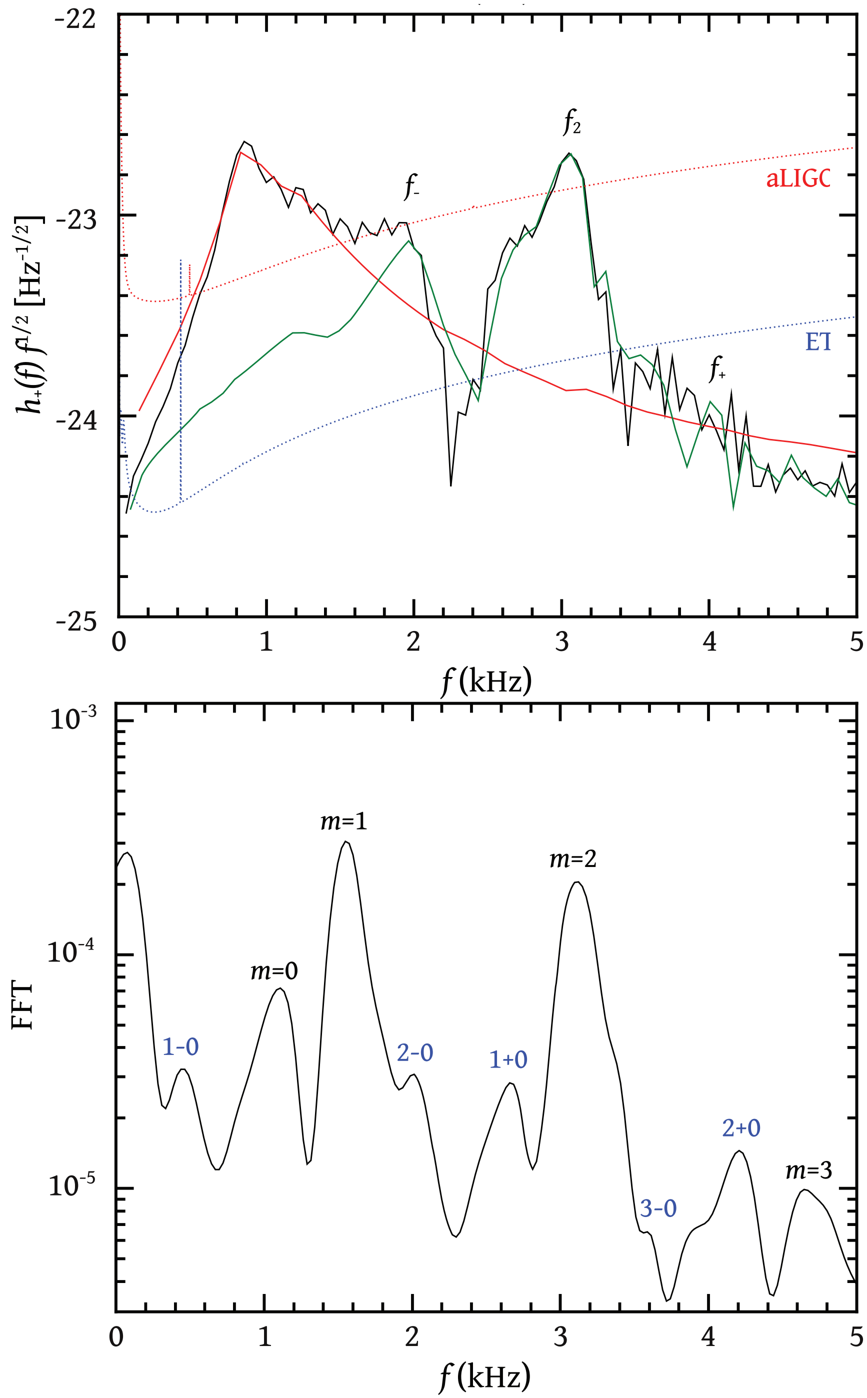

Eigenfunction Extraction

(NS, Apostolatos, Font, 2004)

Fourier extraction of axisymmetric mode eigenfunctions:

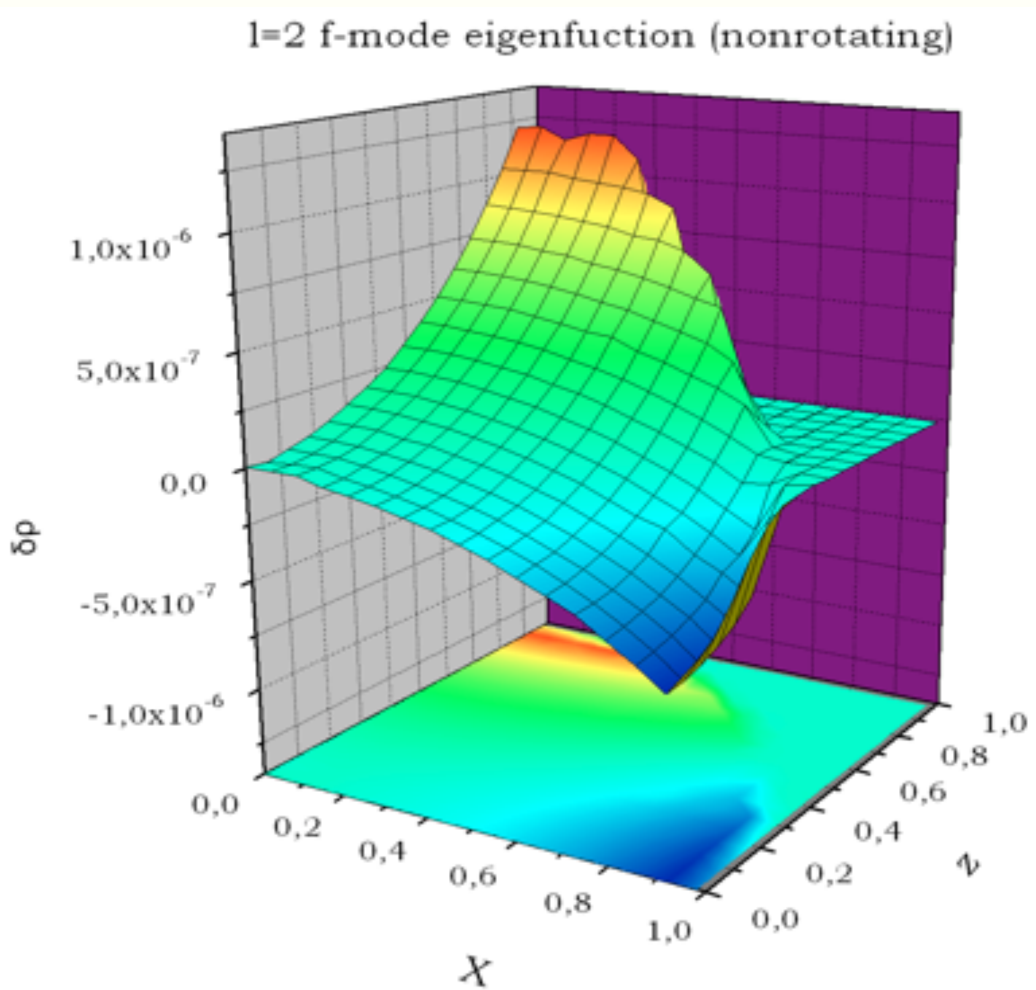

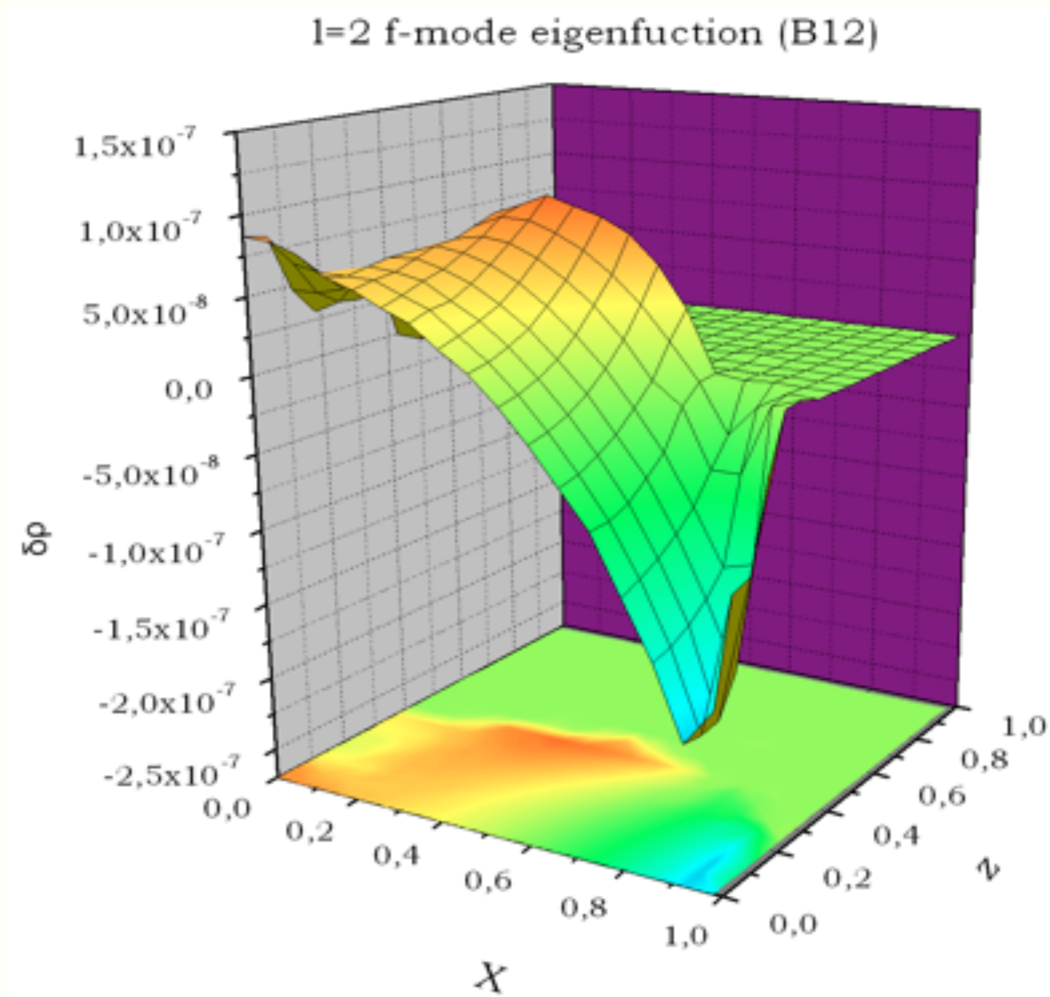

Spatial distribution of FFT *magnitude* at mode-frequency determines shape of *eigenfunction* (but change sign at nodal lines).

Eigenfunctions in Equatorial Plane

m=0, 2, 4 (Shen $1.35M_{sun}+1.35M_{sun}$) m=1 (MIT60 $1.2M_{sun}+1.35M_{sun}$)

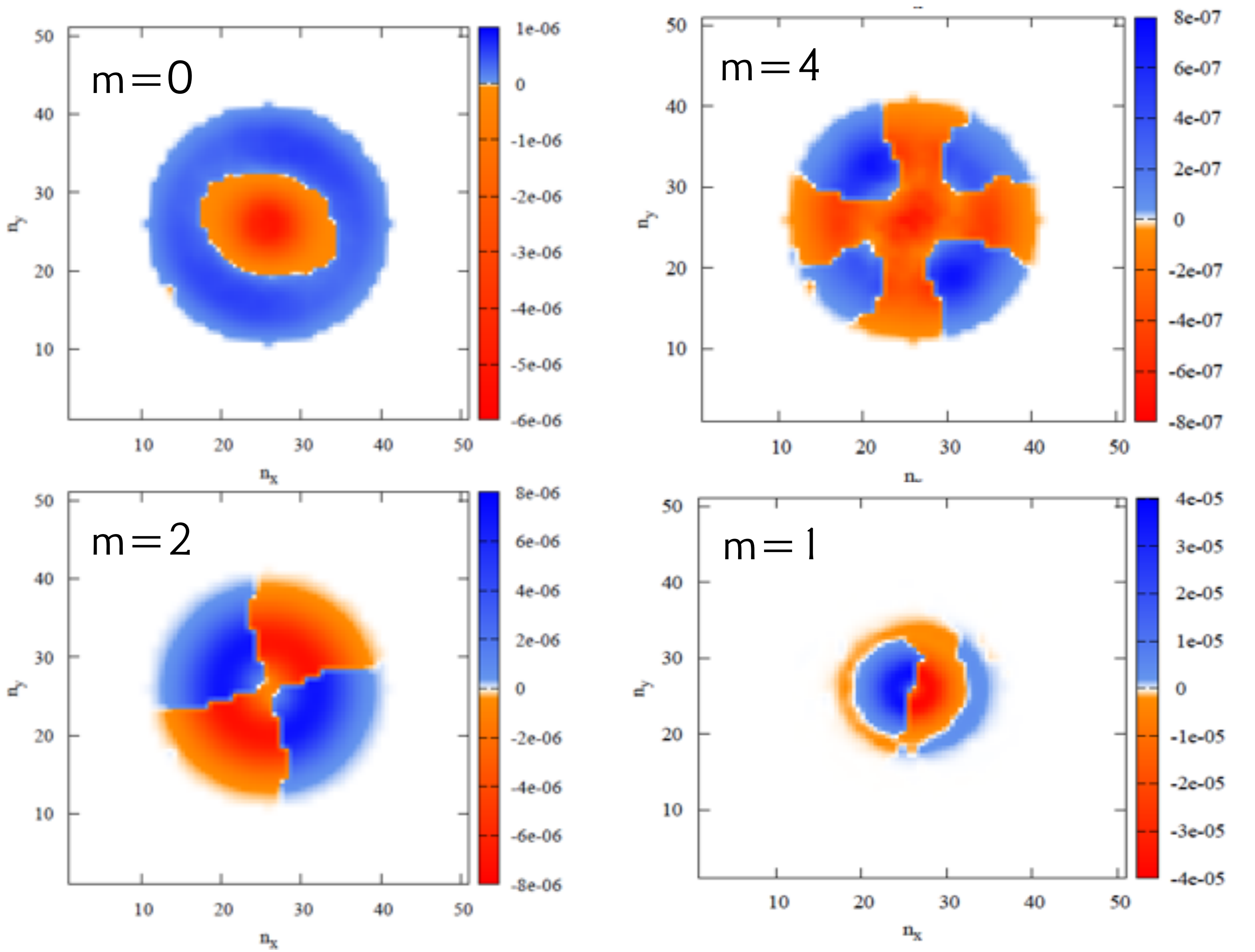

Summary and Prospects

A HMNS created in a binary neutron star merger oscillates in several frequencies with initially high amplitude.

A triplet of frequencies f_-, f_2, f_+ is prominent and potentially detectable.

Identification:

f_2 : m=2 mode

f_- : (m=2) - (m=0) nonlinear combination frequency

In case of detection: determine both m=0 and m=2 frequencies

In progress: construct axisymmetric equilibrium model of HMNS remnant and obtain linear oscillation modes.

PART II:

EXTRACTING EOS INFORMATION

Revealing the EOS

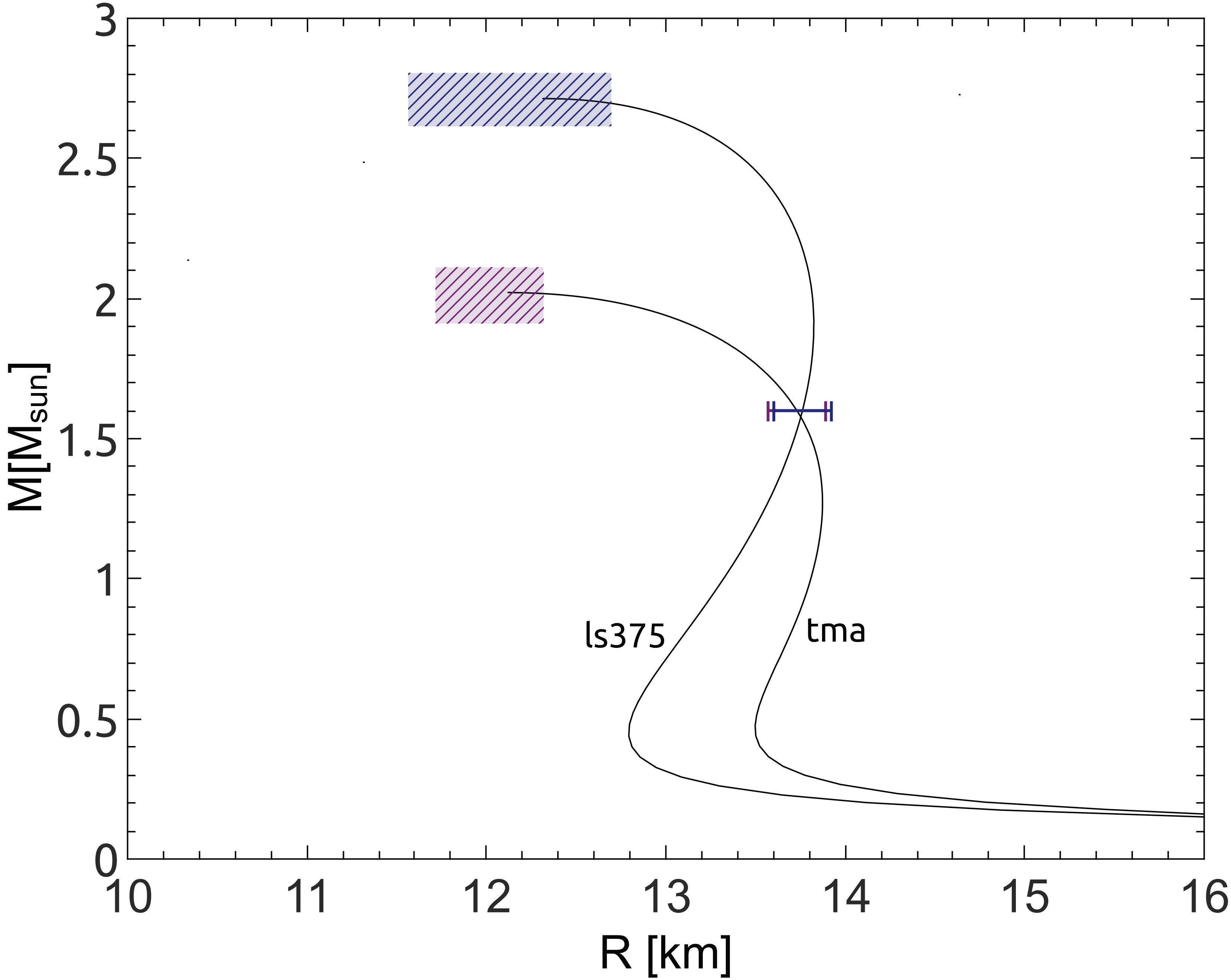

Large EOS Sample

Bauswein, Janka, Hebeler & Schwenk (2012)

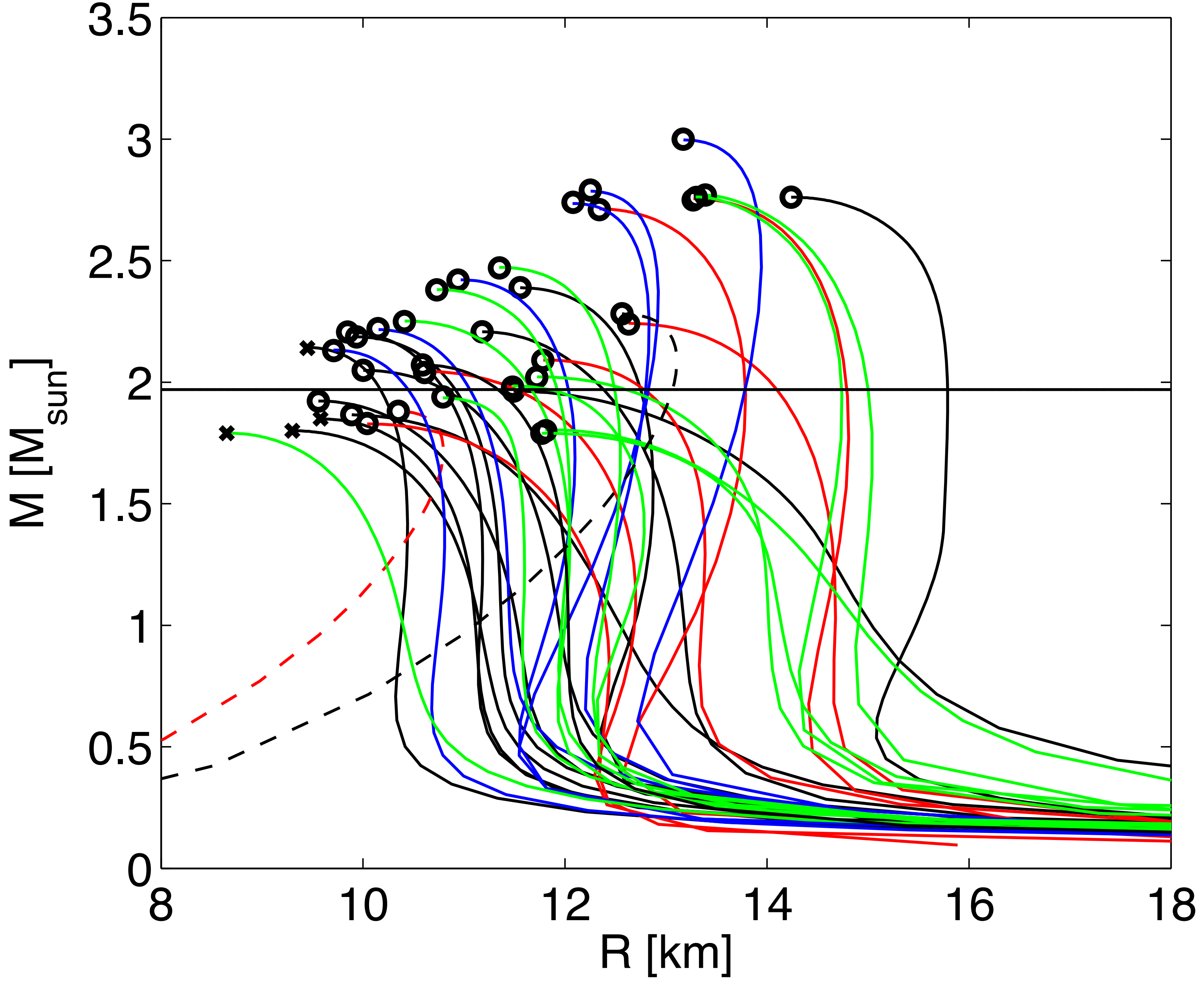

Radius Determination from Post-Merger Signal

Bauswein, Janka, Hebeler & Schwenk (2012)

f_2 correlates well with the radius @ 1.6 Msun, if (M_1, M_2) are known from inspiral.

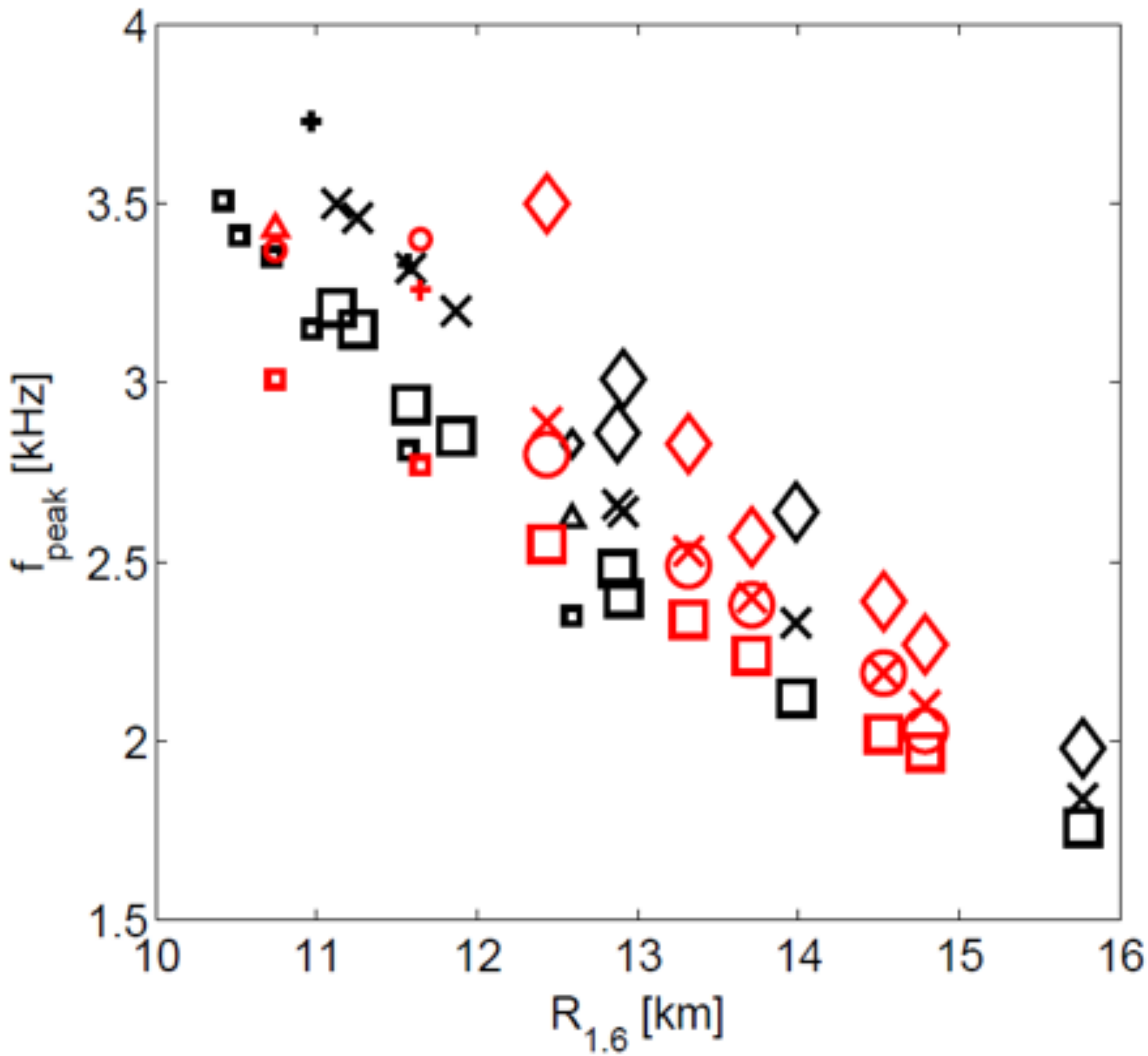

red: 2D EOS

black: cold EOS + Γ=2 thermal part

□ = 1.2+1.2

X, + = 1.35+1.35

O = 1.25+1.5

◇ = 1.5+1.5

Radius Determination from Post-Merger Signal

Bauswein, Janka, Hebeler & Schwenk (2012)

f_2 correlates well with the radius @ 1.6 Msun, if (M_1, M_2) are known from inspiral.

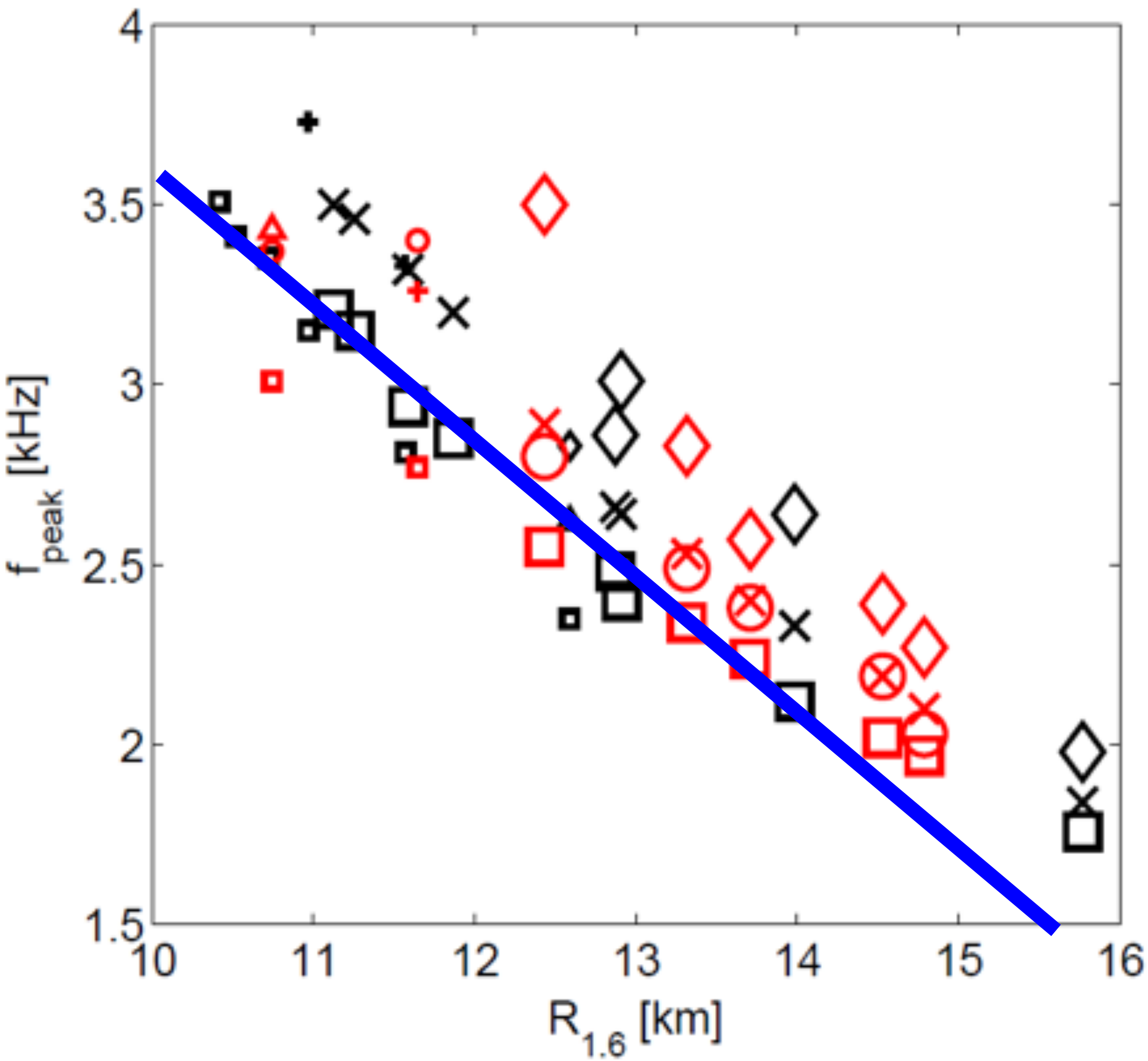

red: 2D EOS

black: cold EOS + Γ=2 thermal part

□ = 1.2+1.2

X, + = 1.35+1.35

O = 1.25+1.5

◇ = 1.5+1.5

Radius Determination from Post-Merger Signal

Bauswein, Janka, Hebeler & Schwenk (2012)

f_2 correlates well with the radius @ 1.6 Msun, if (M_1, M_2) are known from inspiral.

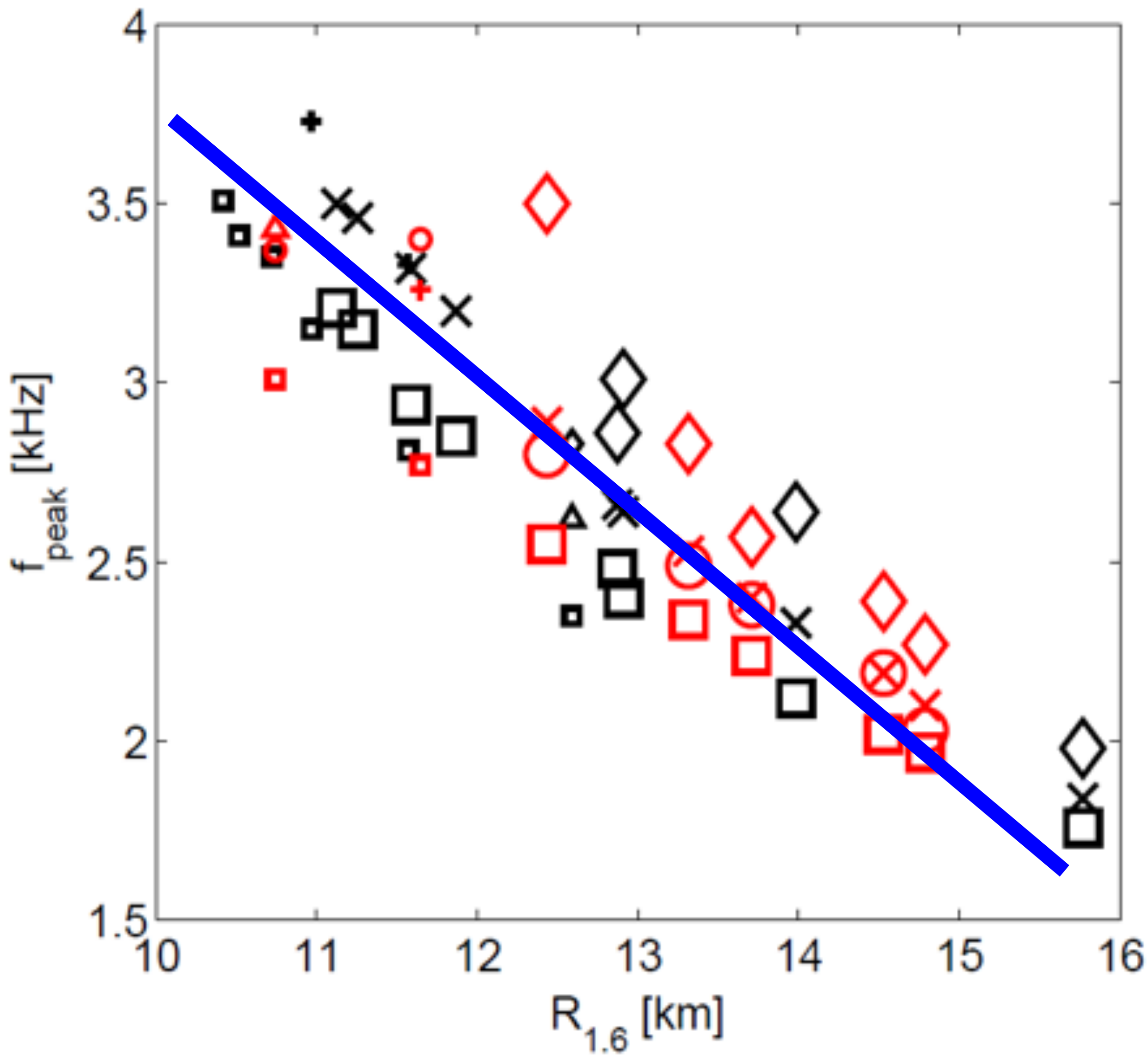

red: 2D EOS

black: cold EOS + Γ=2 thermal part

□ = 1.2+1.2

X, + = 1.35+1.35

O = 1.25+1.5

◇ = 1.5+1.5

Radius Determination from Post-Merger Signal

Bauswein, Janka, Hebeler & Schwenk (2012)

f_2 correlates well with the radius @ 1.6 Msun, if (M_1, M_2) are known from inspiral.

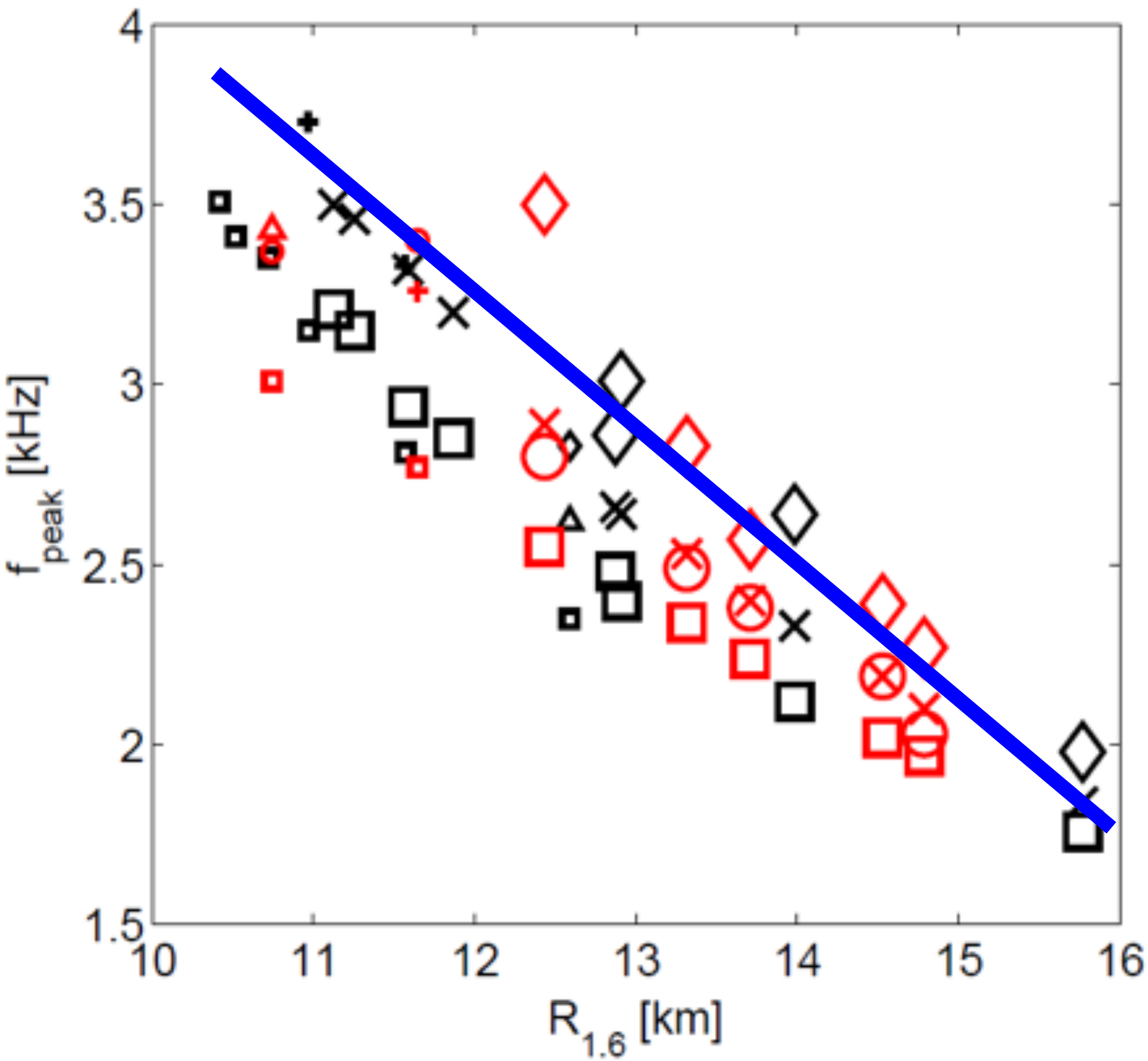

red: 2D EOS

black: cold EOS + Γ=2 thermal part

□ = 1.2+1.2

X, + = 1.35+1.35

O = 1.25+1.5

◇ = 1.5+1.5

Radius Determination from Post-Merger Signal

Bauswein, Janka, Hebeler & Schwenk (2012)

For 1.35+1.35 Msun the empirical relation is remarkably accurate.

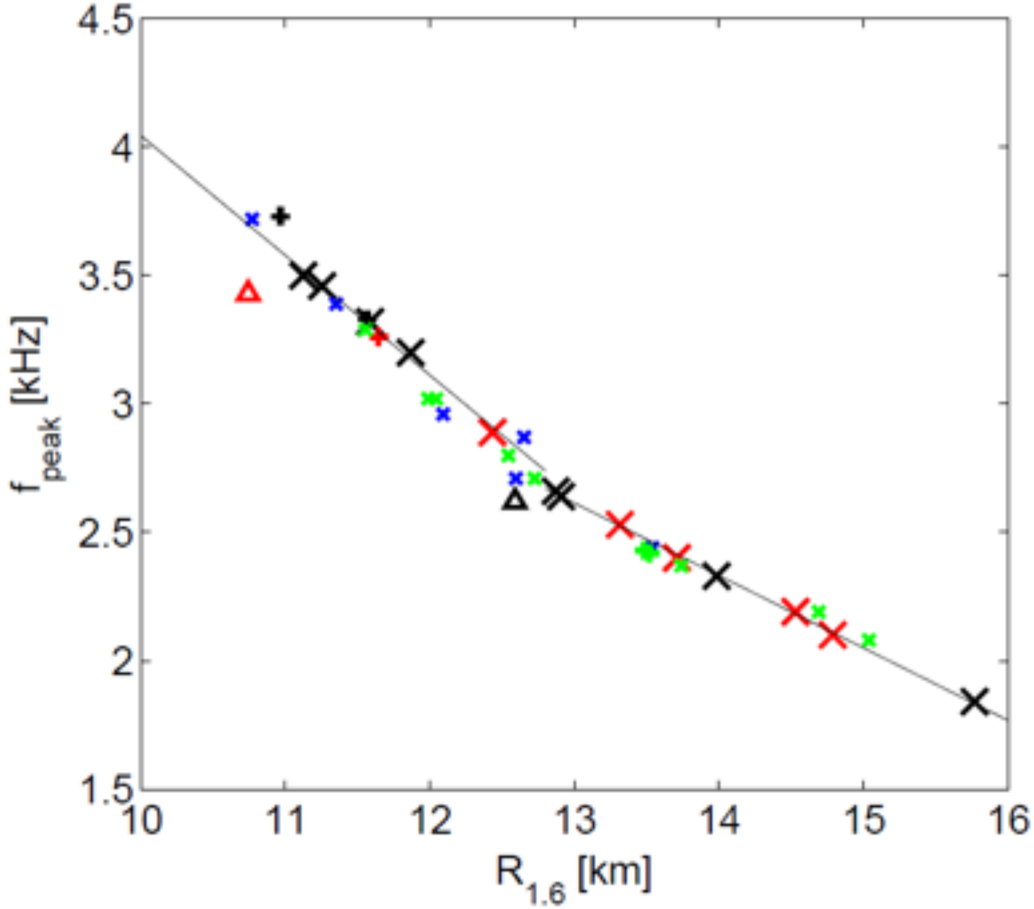

$$f_{peak} = \begin{cases} -0.2823 \cdot R_{1.6} + 6.284 & \text{for } f_{peak} < 2.8 \text{ kHz} \\ -0.4667 \cdot R_{1.6} + 8.713 & \text{for } f_{peak} > 2.8 \text{ kHz} \end{cases}$$

Radius Determination from Post-Merger Signal

Bauswein, Janka, Hebeler & Schwenk (2012)

For given 1.35+1.35 Msun:

f_2 correlates with $R_{remnant}$
$R_{remnant}$ is proportional to $R_{1.6}$
=> f_2 correlates with $R_{1.6}$

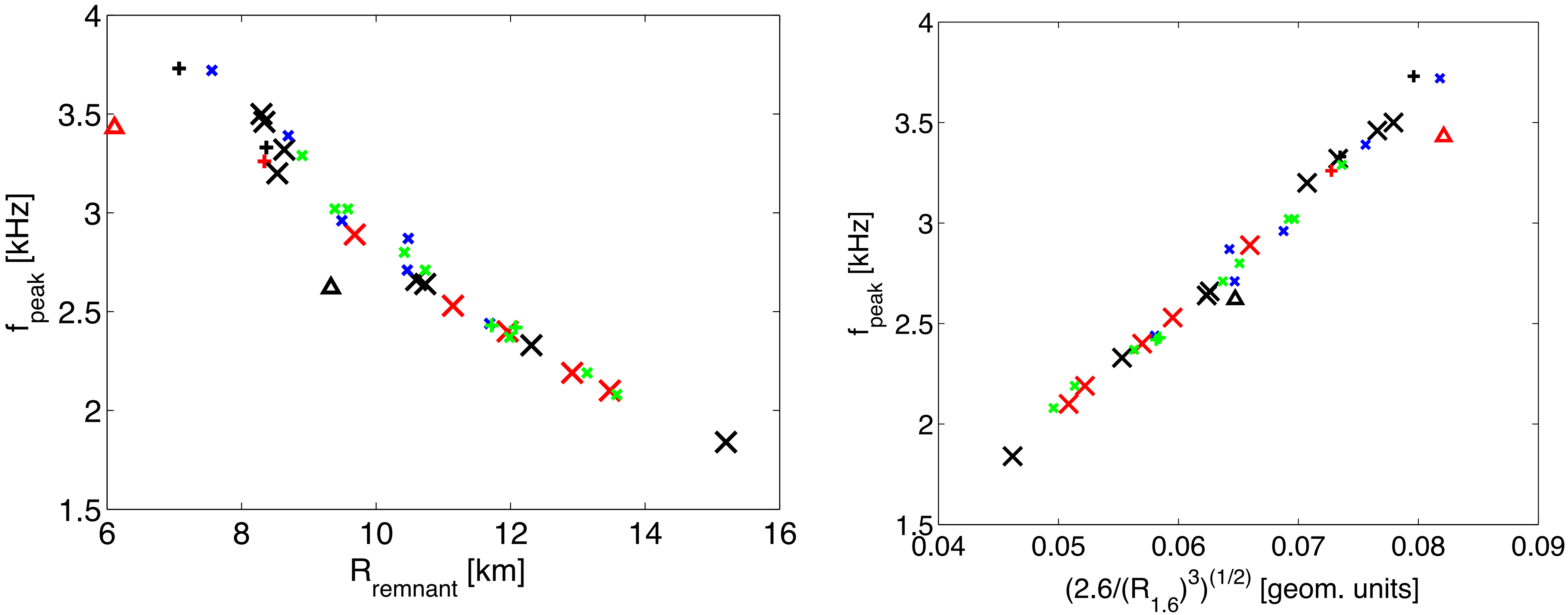

Extrapolating to larger masses

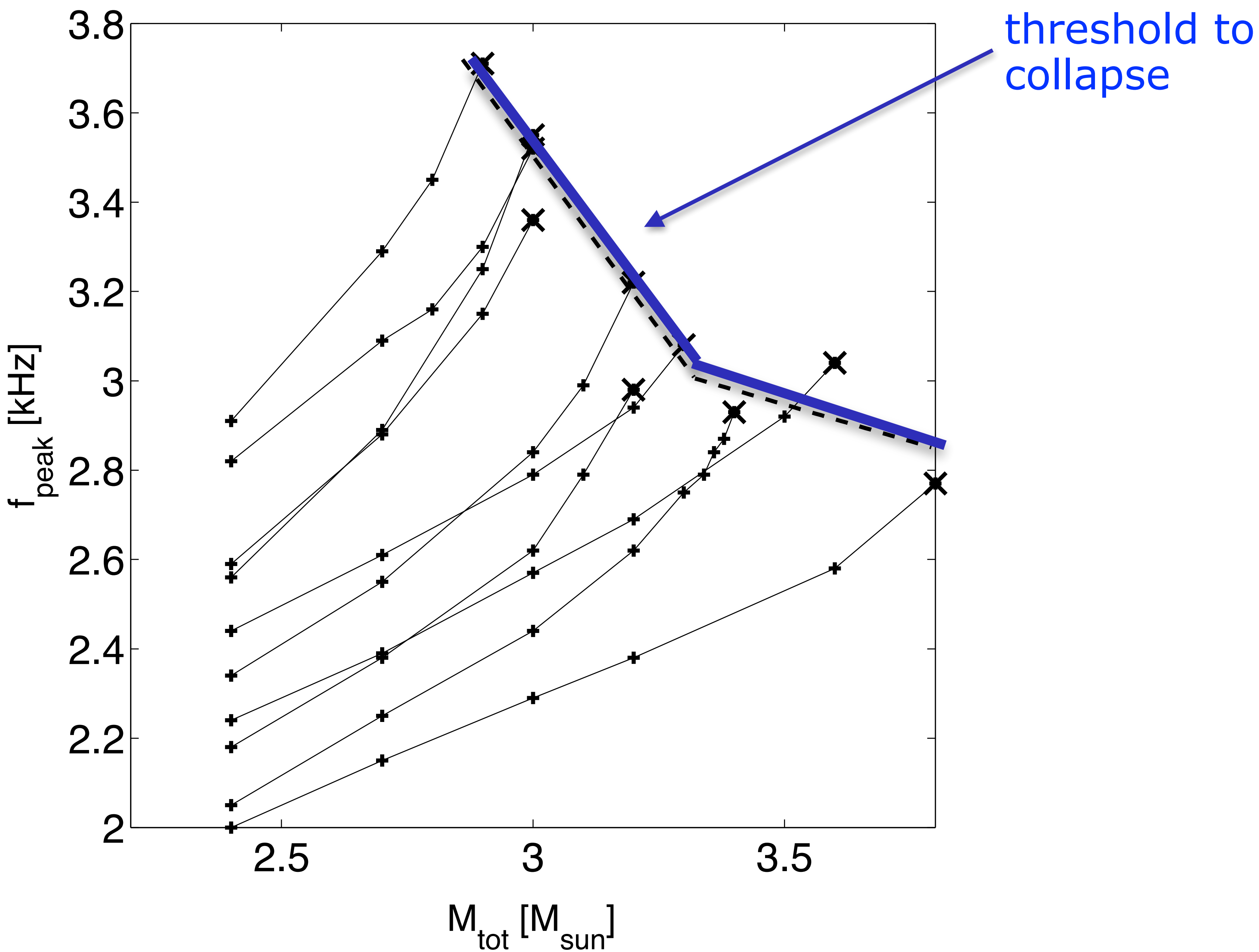

Extrapolating to larger masses

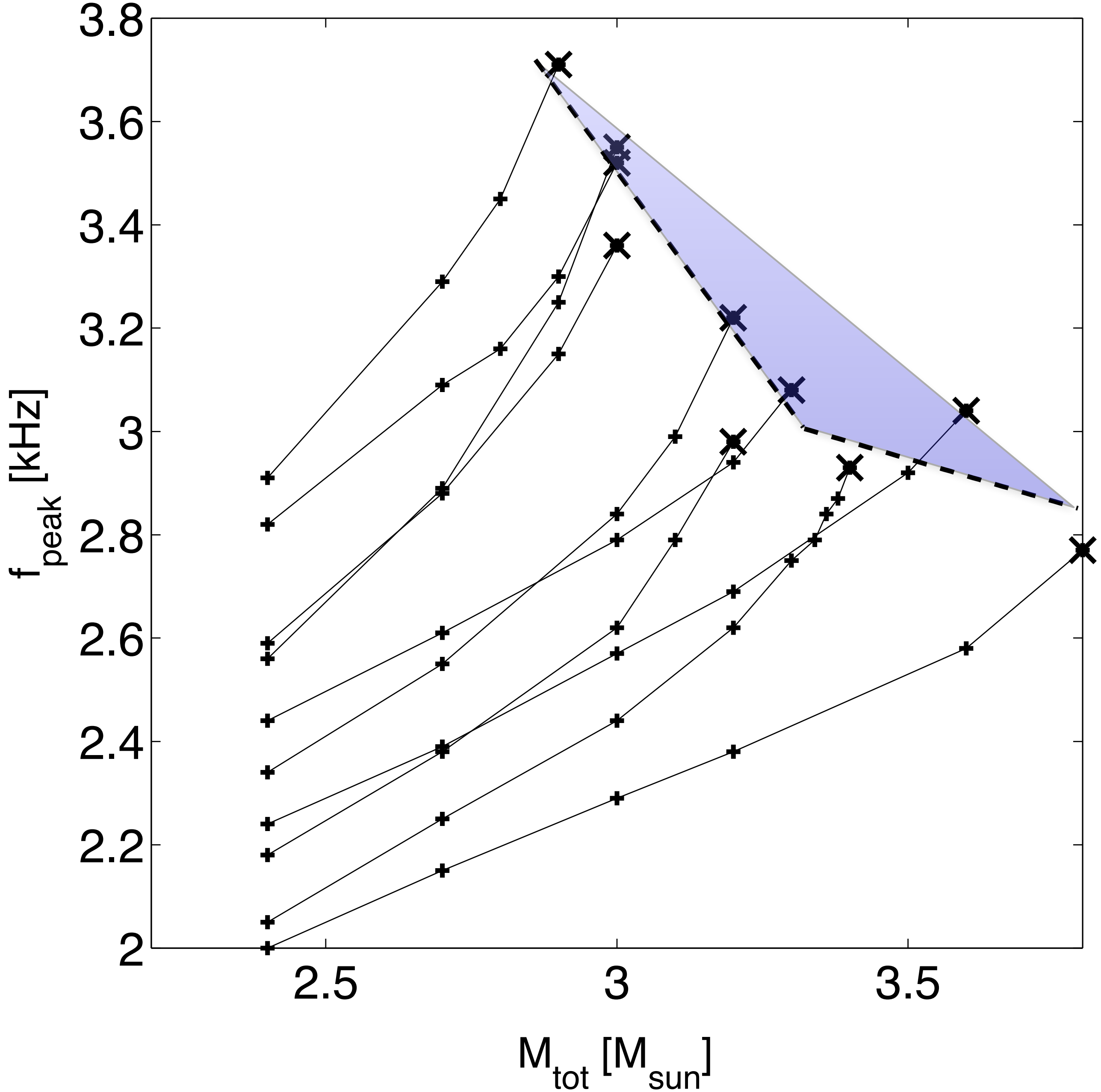

Extrapolating to larger masses

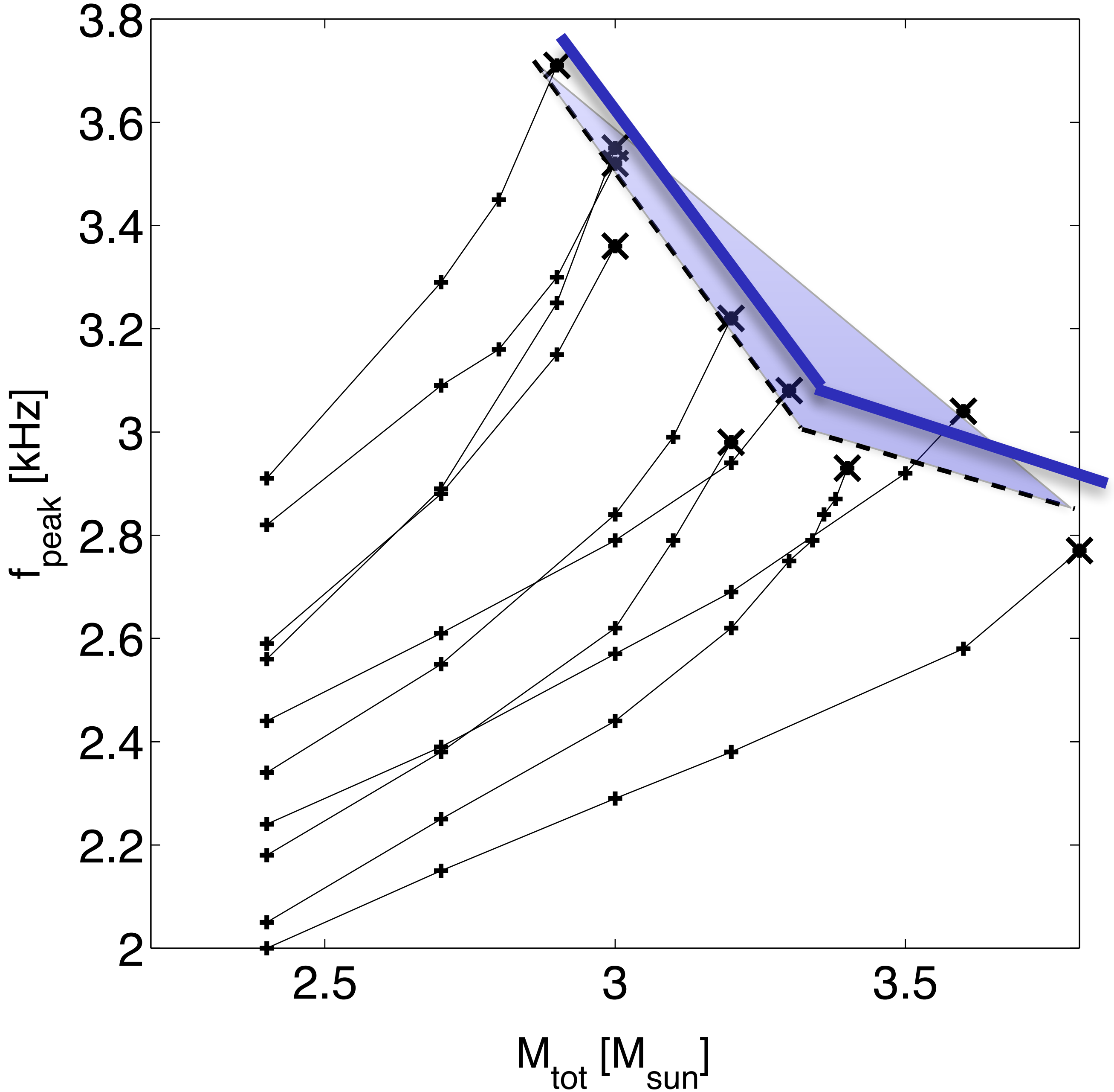

Extrapolating to larger masses

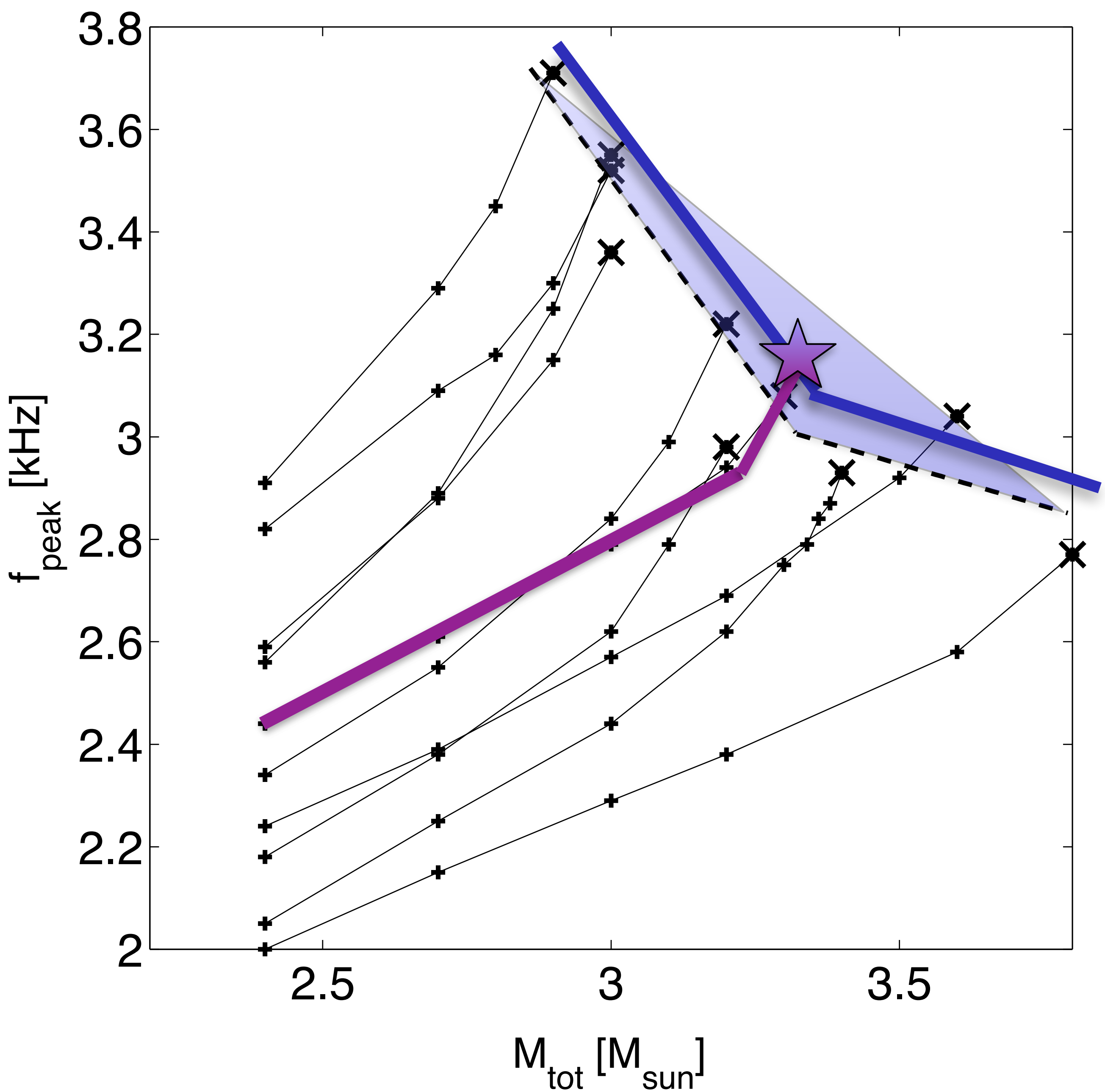

Extrapolating to larger masses

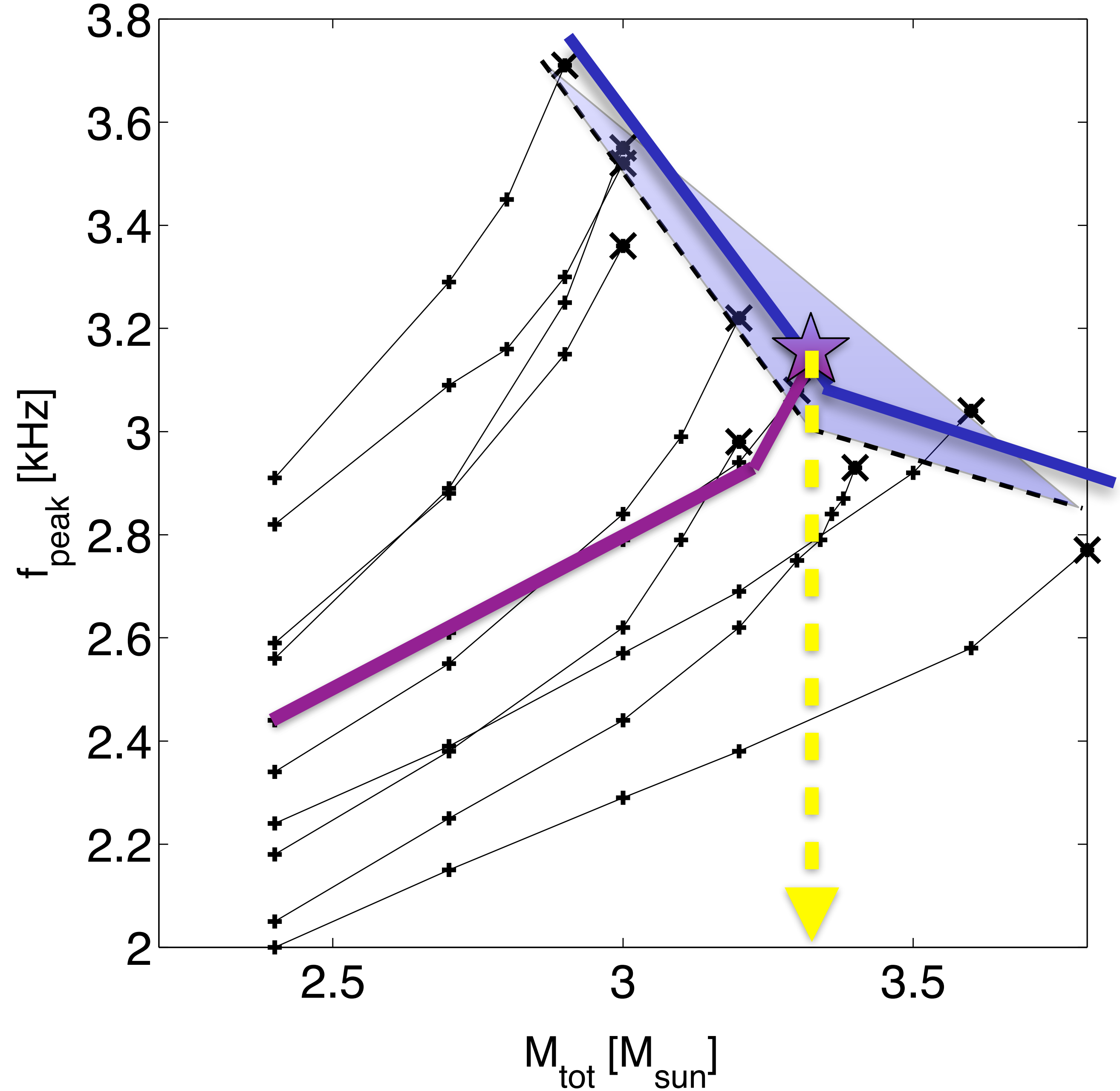

Extrapolating to larger masses

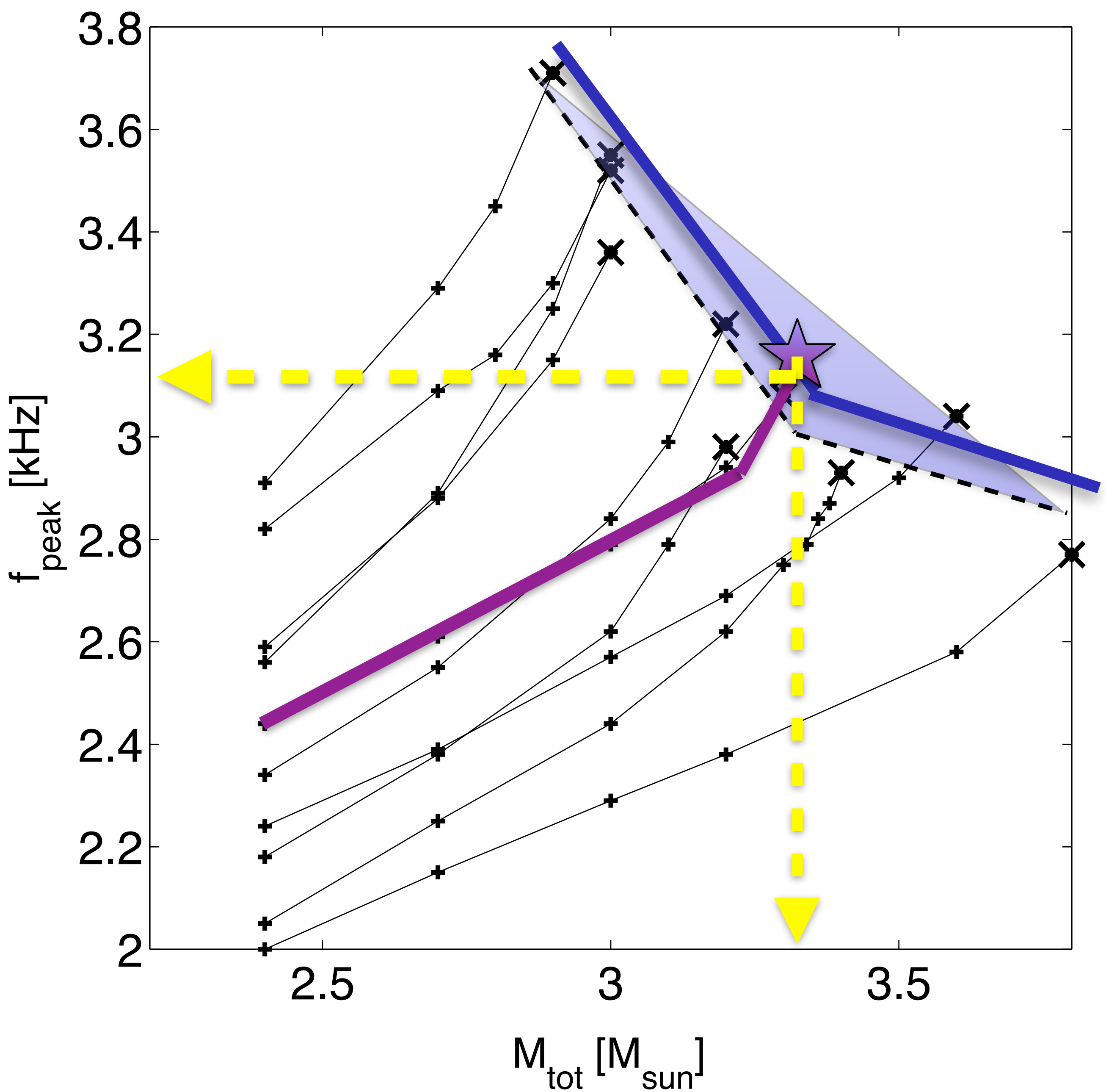

M_{thres} vs. M_{max} correlation

Bauswein, Baumgarte, Janka PRL (2013)

The threshold mass is related to the maximum TOV mass as

$$M_{\rm thres} = k \cdot M_{\rm max}$$

where k is dependent on the compactness.

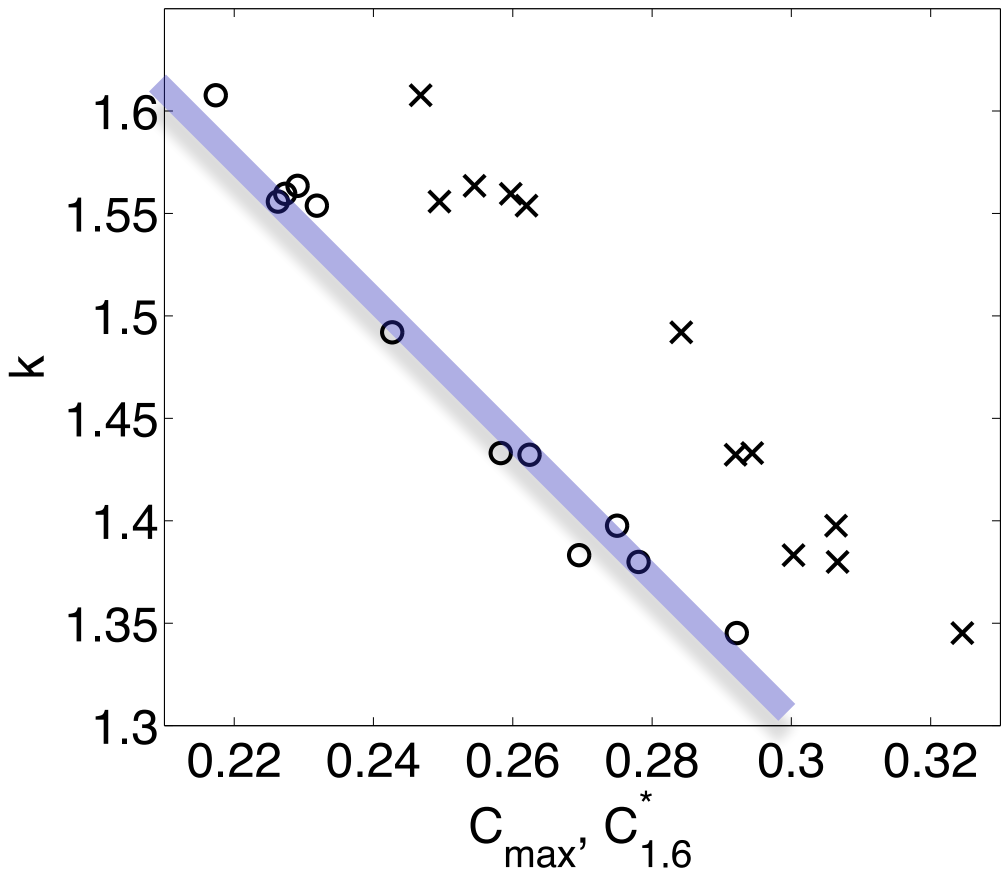

$$C_{\rm max} = (GM_{\rm max})/(c^2 R_{\rm max})$$

M_{thres} vs. M_{max} correlation

Bauswein, Baumgarte, Janka PRL (2013)

The threshold mass is related to the maximum TOV mass as

$$M_{\mathrm{thres}} = k \cdot M_{\mathrm{max}}$$

where k is dependent on the compactness.

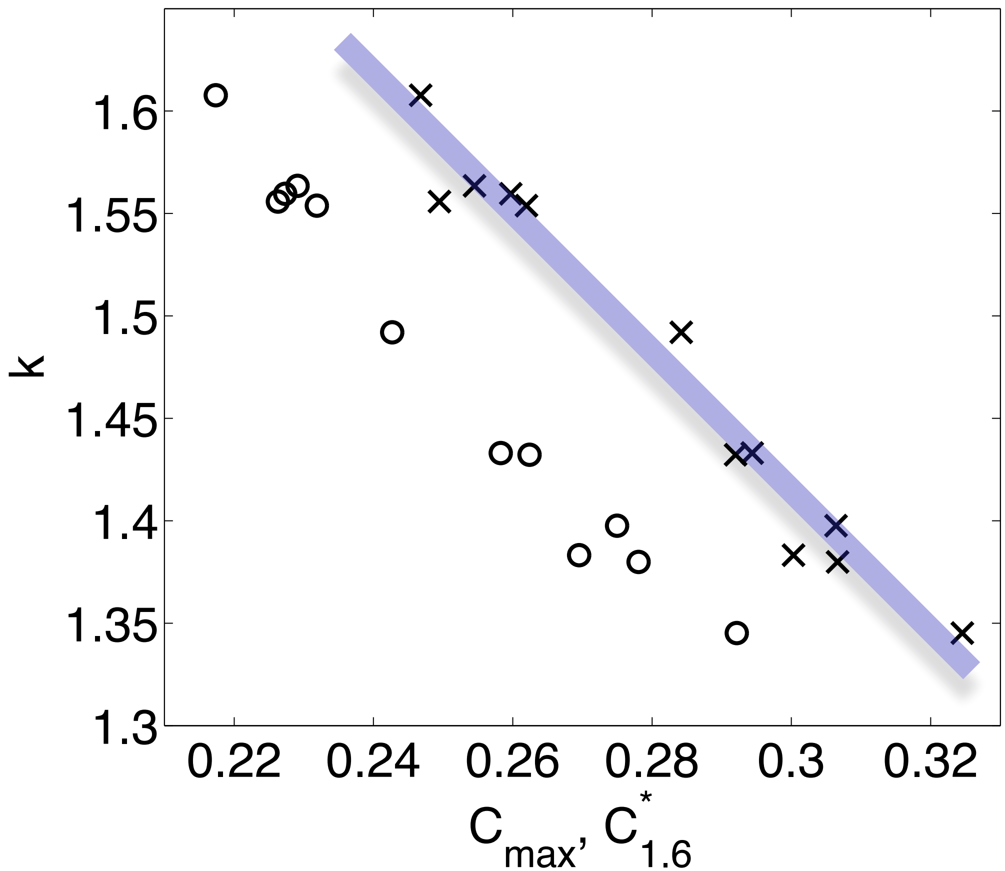

$$C^*_{1.6} = (GM_{\mathrm{max}})/(c^2 R_{1.6})$$

f_{thres} vs. R_{max} correlation

At $M_{tot} \sim 2.7\ M_{sun}$

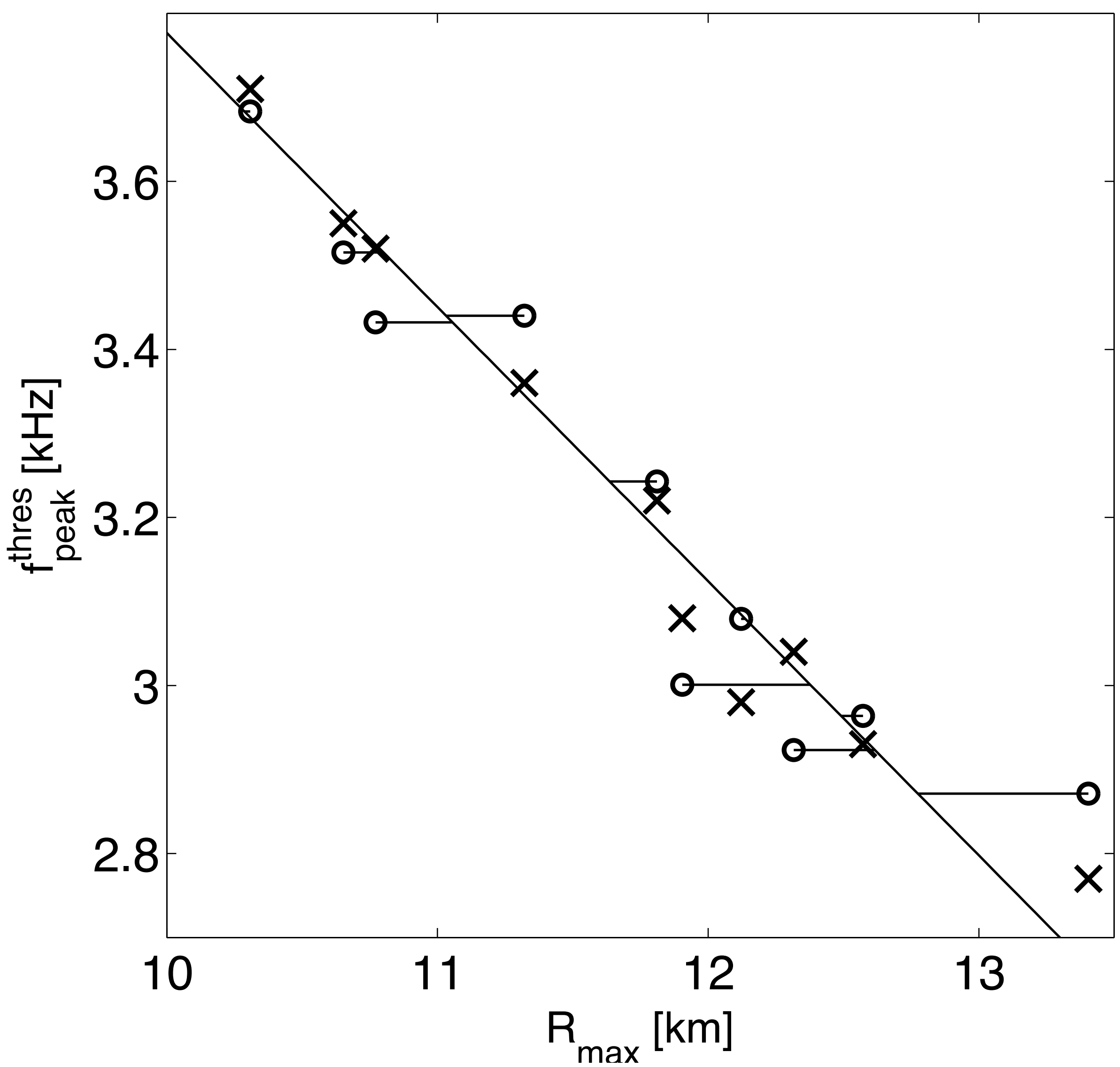

Largest error bars for maximum mass model

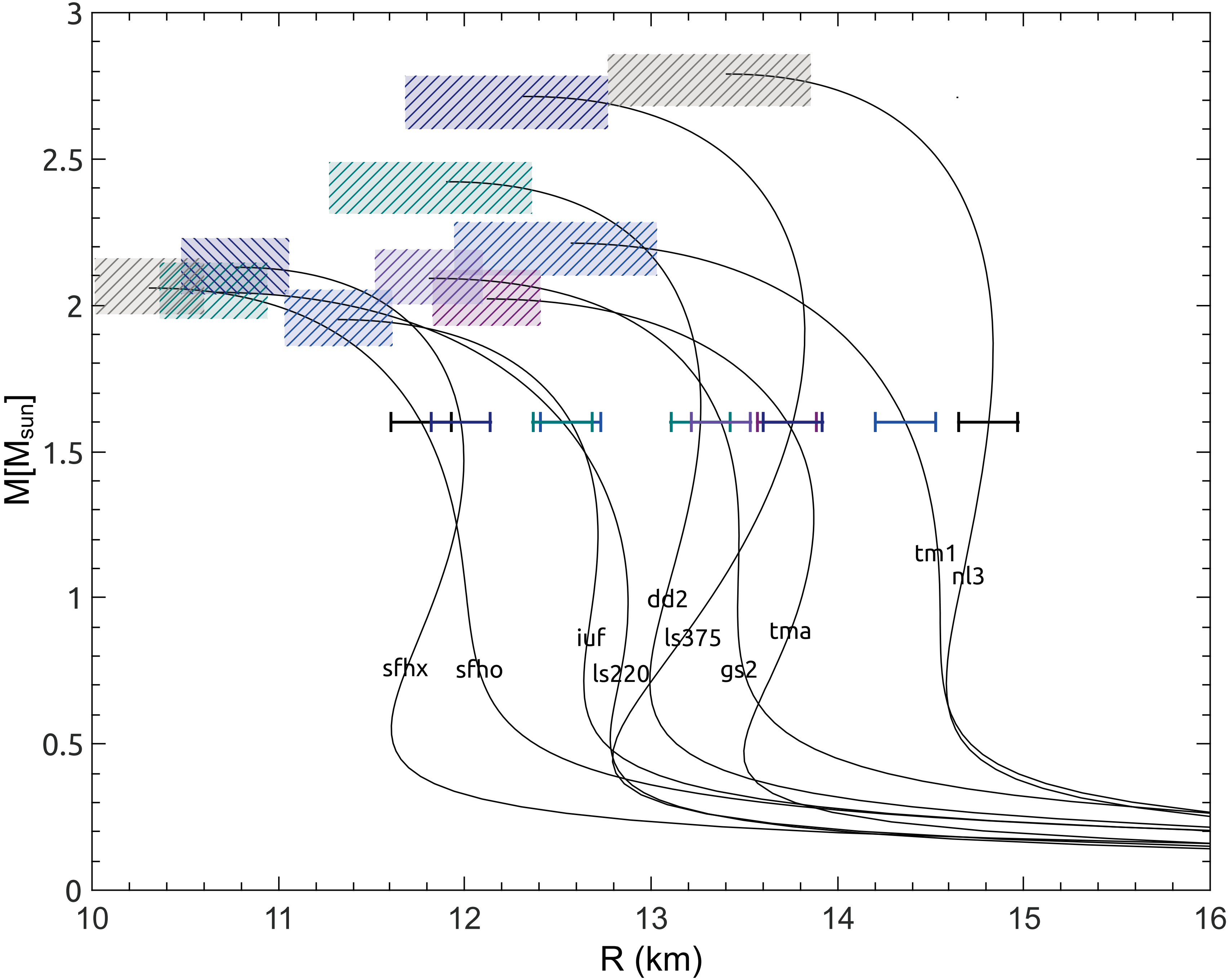

Breaking the EOS degeneracy

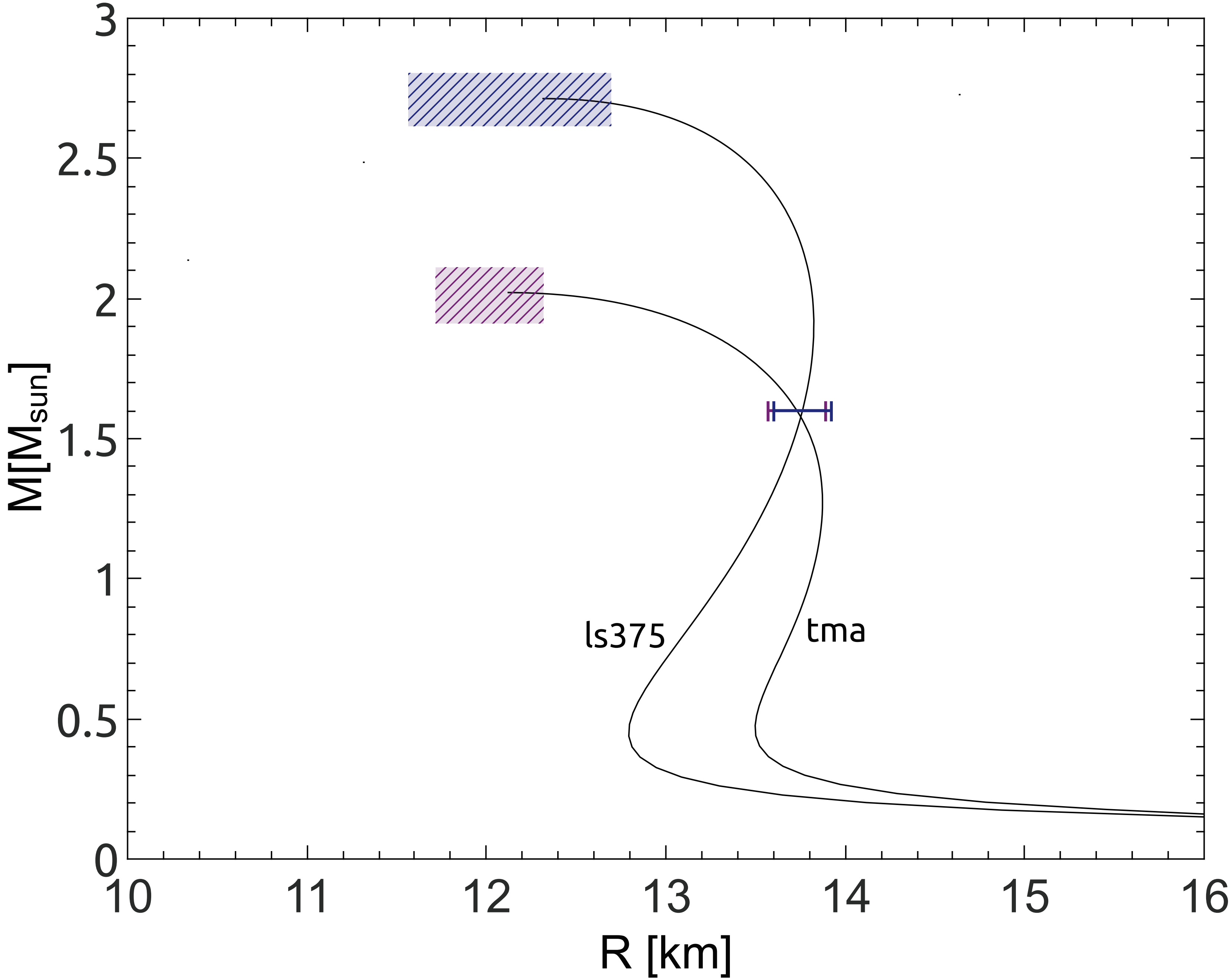

Estimating the density of the maximum-mass model

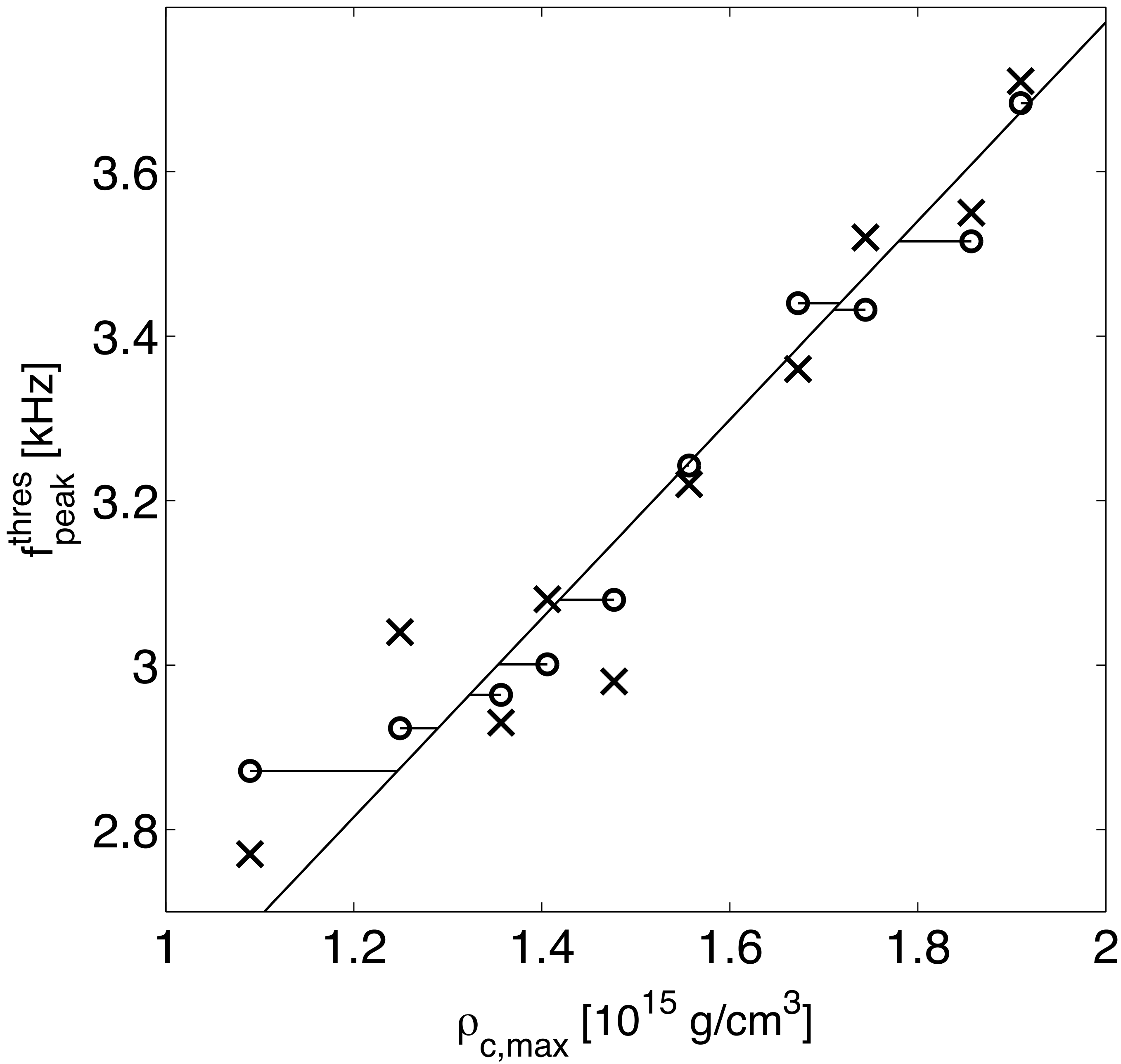

PART III:

TOWARDS HYBRID WAVEFORMS

GW damping timescale for f-modes

Andersson & Kokkotas (1998)

No rotation: EOS-independent empirical relation:

$$\frac{1}{\tau_0[\mathrm{s}]} = \frac{\bar{M}^3}{\bar{R}^4}\left[22.85 - 14.65\frac{\bar{M}}{\bar{R}}\right]$$

When this is applied to the mass and radius of the remnant:

$\tau \sim 200$ ms.

f-modes of rapidly rotating neutron stars

Doneva, Gaertig, Kokkotas, Krueger (2013)

Uniform rotation, Cowling approximation, $l=\pm m=2$ *f*-mode frequency (linear time-evolution code)

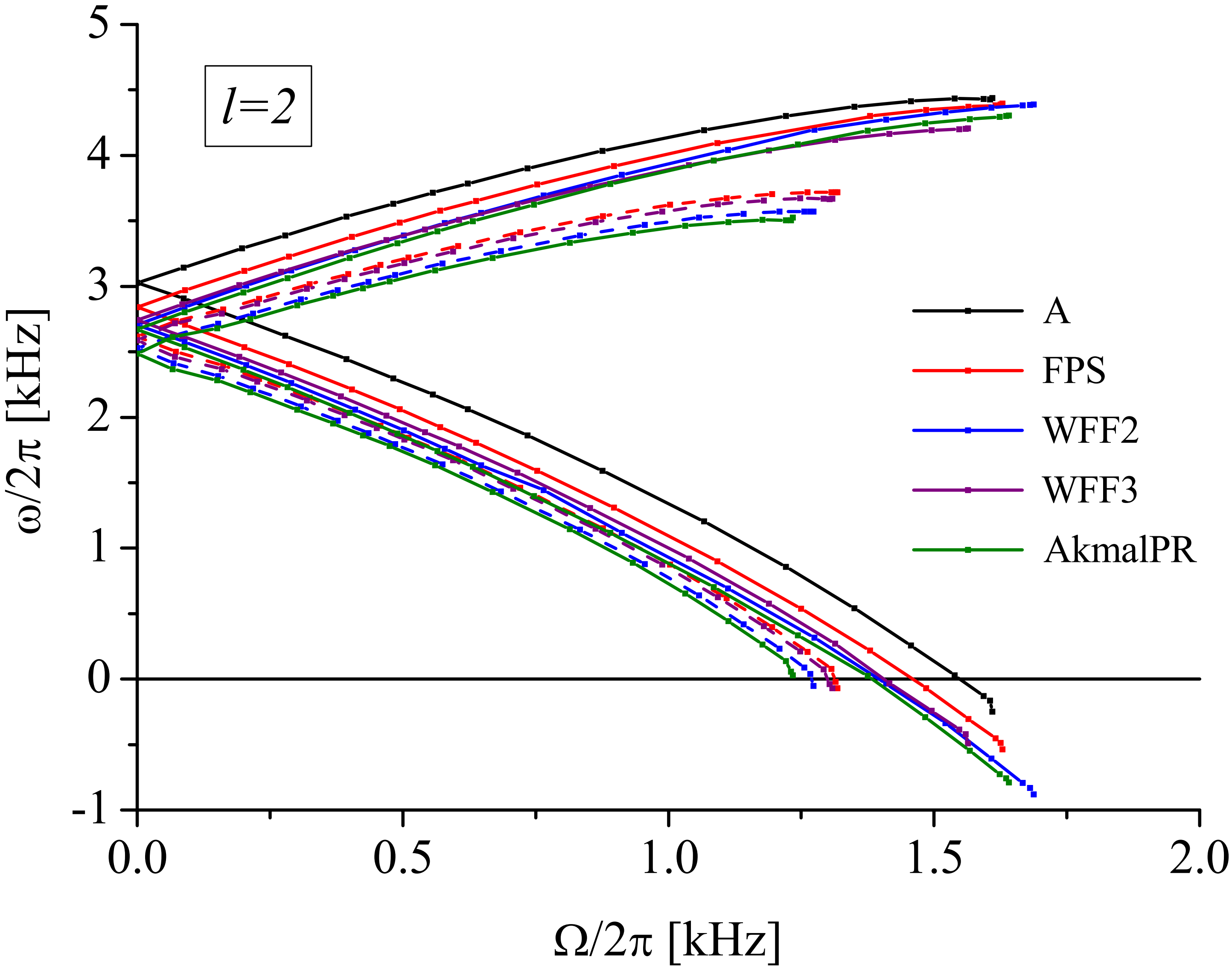

f-modes of rapidly rotating neutron stars

Doneva, Gaertig, Kokkotas, Krueger (2013)

Corotating frame: same rotational effect, independent of EOS!

→ Empirical relations for GW asteroseismology.

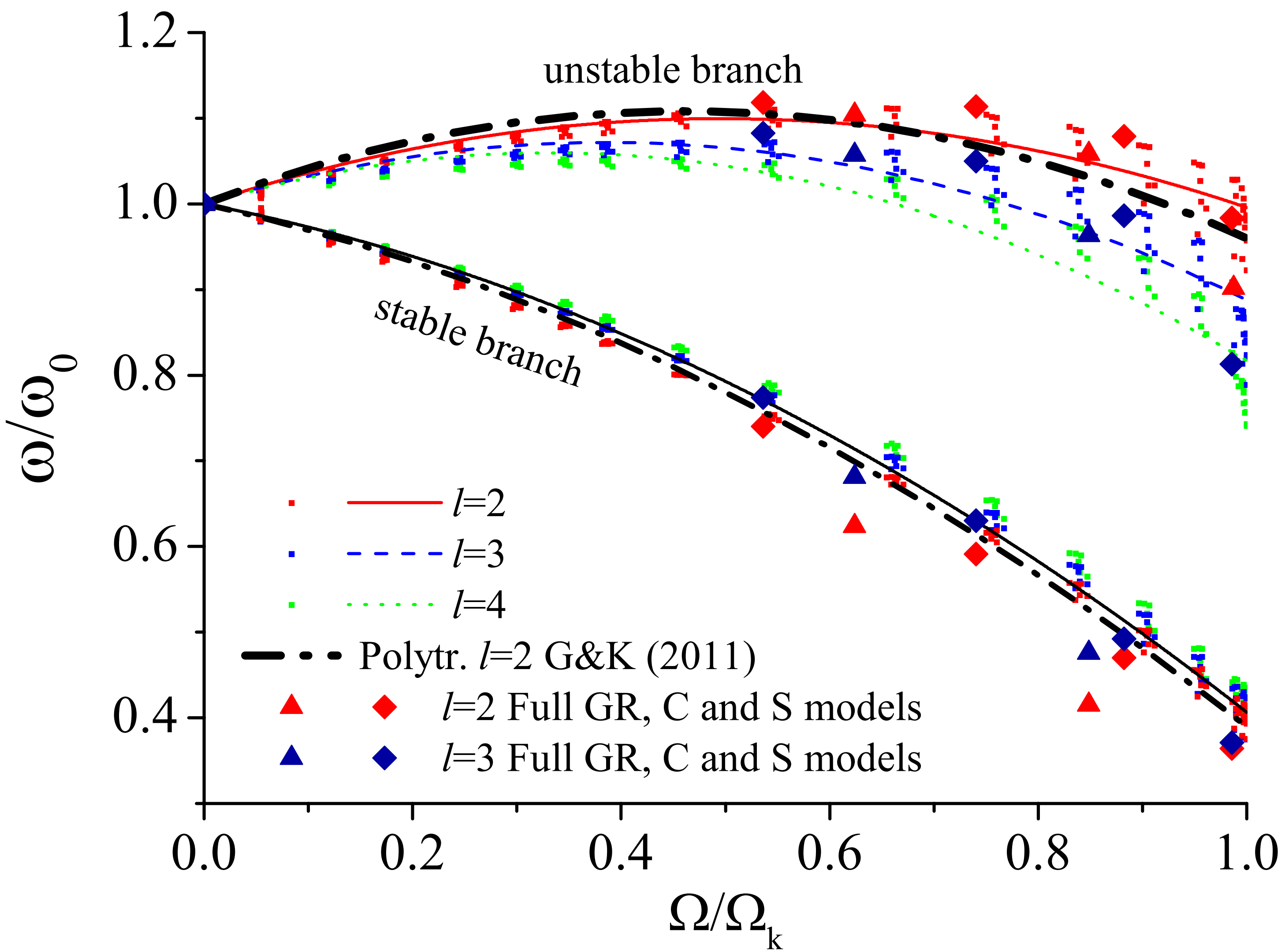

GW damping timescale for f-modes

Doneva, Gaertig, Kokkotas, Krueger (2013)

Uniform rotation: same rotational effect, independent of EOS!

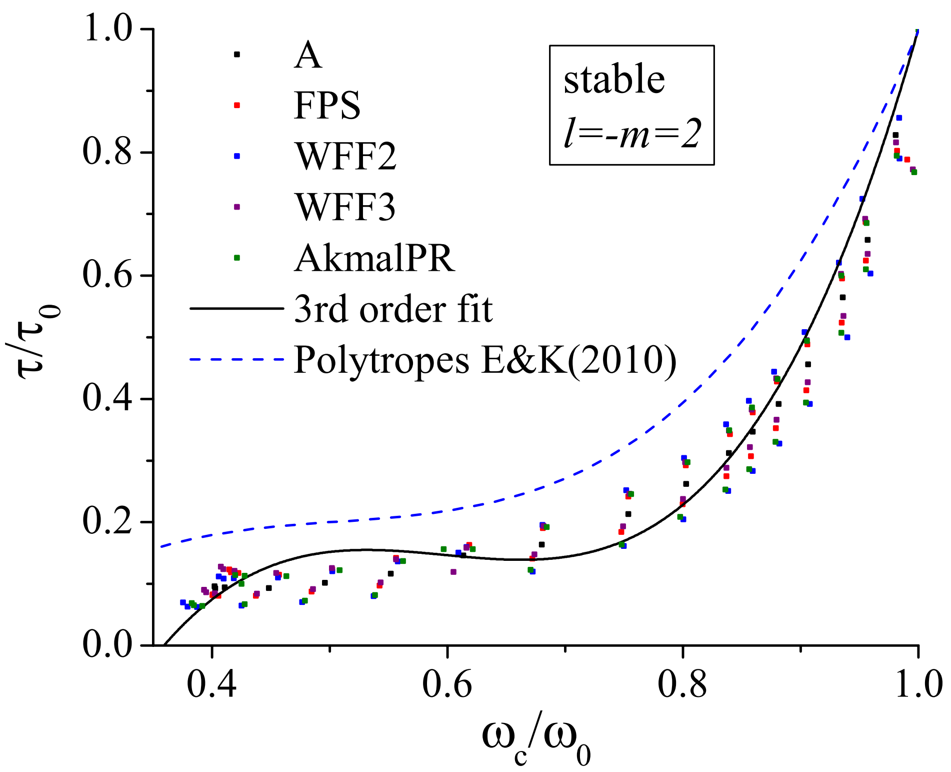

At rapid rotation: we estimate

$\tau \sim \tau_0/10$ i.e. ~ 20 ms.

Real GW timescale is probably

20ms < τ <200ms -> work in progress!

THANK YOU

SUPPLEMENTARY MATERIAL

TABLE I: Equation of state models with references and resulting stellar properties. $M_{\rm max}$ denotes the maximum mass of nonrotating NSs with the cirumferential radius $R_{\rm max}$ corresponding this maximum-mass configuration. $e_{\rm max}$ and $\rho_{\rm max}$ are the central energy density and the central rest-mass density of the maximum-mass configuration. $R_{1.6}$ refers to the circumferential radius of a nonrotating 1.6 $M_\odot$ NS. $M_{\rm thres}$ is the highest total binary mass which leads to differentially rotating NS merger remnant for the given EoS. The dominant GW frequency of this postmerger remnant is $f_{\rm peak}^{\rm thres}$. Hatted quantities are the estimates for these merger properties and stellar parameters based on the extrapolation procedure described in the main text (Sect. IV).

EoS	$M_{\rm max}$ ($M_\odot$)	$\hat{M}_{\rm max}$ ($M_\odot$)	$R_{1.6}$ (km)	$\hat{R}_{1.6}$ (km)	$M_{\rm thres}$ ($M_\odot$)	$\hat{M}_{\rm thres}$ ($M_\odot$)	$f_{\rm peak}^{\rm thres}$ (kHz)	$\hat{f}_{\rm peak}^{\rm thres}$ (kHz)	$R_{\rm max}$ (km)	$\hat{R}_{\rm max}$ (km)	$e_{\rm c,max}$ (g/cm^3)	$\hat{e}_{\rm c,max}$ (g/cm^3)	$\rho_{\rm c,max}$ (g/cm^3)	$\hat{\rho}_{\rm c,max}$ (g/cm^3)
NL3 [70, 71]	2.79	2.68	14.81	14.72	3.8	3.73	2.77	2.87	13.40	12.78	1.52×10^{15}	1.68×10^{15}	1.09×10^{15}	1.25×10^{15}
LS375 [73]	2.71	2.69	13.76	13.86	3.6	3.57	3.04	2.93	12.32	12.62	1.78×10^{15}	1.74×10^{15}	1.25×10^{15}	1.29×10^{15}
DD2 [71, 74]	2.42	2.40	13.26	13.18	3.3	3.33	3.08	3.00	11.90	12.38	1.95×10^{15}	1.83×10^{15}	1.41×10^{15}	1.35×10^{15}
TM1 [68, 69]	2.21	2.28	14.36	14.34	3.4	3.45	2.93	2.96	12.57	12.49	1.80×10^{15}	1.79×10^{15}	1.36×10^{15}	1.32×10^{15}
SFHX [75]	2.13	2.19	11.98	12.07	3.0	3.05	3.52	3.43	10.77	11.06	2.39×10^{15}	2.33×10^{15}	1.74×10^{15}	1.71×10^{15}
GS2 [76]	2.09	2.07	13.38	13.35	3.2	3.17	3.22	3.24	11.81	11.64	2.05×10^{15}	2.11×10^{15}	1.56×10^{15}	1.55×10^{15}
SFHO [75]	2.06	1.97	11.77	11.76	2.9	2.88	3.71	3.68	10.31	10.29	2.67×10^{15}	2.63×10^{15}	1.91×10^{15}	1.92×10^{15}
LS220 [73]	2.04	1.98	12.52	12.47	3.0	2.99	3.55	3.52	10.65	10.80	2.55×10^{15}	2.43×10^{15}	1.86×10^{15}	1.78×10^{15}
TMA [69, 77]	2.02	2.12	13.73	13.89	3.2	3.27	2.98	3.08	12.12	12.14	1.92×10^{15}	1.92×10^{15}	1.48×10^{15}	1.42×10^{15}
IUF [71, 78]	1.95	2.05	12.57	12.50	3.0	3.04	3.36	3.44	11.32	11.03	2.19×10^{15}	2.34×10^{15}	1.67×10^{15}	1.72×10^{15}

ACCURACY OF IWM-CFC APPROXIMATION

Iosif, Stergioulas, arXiv:1406.7375 (2014)